Flat-band generator in two dimensions

Wulayimu Maimaiti,[1,2,3] Alexei Andreanov,[1,2] and Sergej Flach[1,2]
[1]*Center for Theoretical Physics of Complex Systems, Institute for Basic Science(IBS), Daejeon 34126, Korea*
[2]*Basic Science Program(IBS School), Korea University of Science and Technology(UST), Daejeon 34113, Korea*
[3]*Department of Physics and Astronomy, Center for Materials Theory, Rutgers University, Piscataway, New Jersey 08854, USA*

(Received 11 January 2021; accepted 24 March 2021; published 16 April 2021)

Dispersionless bands, flat bands, provide an excellent test bed for novel physical phases due to the fine-tuned character of flat band tight-binding Hamiltonians. The accompanying macroscopic degeneracy makes any perturbation relevant, no matter how small. For short-range hoppings flat-bands support compact localized states, which allowed us to develop systematic flat-band generators in $d = 1$ dimension in Phys. Rev. B **95**, 115135 (2017) and Phys. Rev. B **99**, 125129 (2019). Here we extend this generator approach to $d = 2$ dimensions. The shape of a compact localized state turns into an important additional flat-band classifier. This allows us to obtain analytical solutions for classes of $d = 2$ flat-band networks and to reclassify and reobtain known ones, such as the checkerboard, kagome, Lieb, and Tasaki lattices. Our generator can be straightforwardly generalized to three lattice dimensions as well.

DOI: 10.1103/PhysRevB.103.165116

I. INTRODUCTION

Physical systems with macroscopic degeneracies have attracted a lot of attention during recent decades. Such degeneracies are highly sensitive to even the slightest perturbations, which makes them perfect test beds for identifying and studying various exotic or unconventional correlated phases of matter. Flat bands are dispersionless energy bands of translationally invariant tight-binding networks [1,2]. The absence of dispersion implies a macroscopic degeneracy of the flat-band eigenstates. A flat-band (FB) results from destructive interference of the hoppings, which requires their fine tuning. All the known FB examples with short-range hopping support compact localized states (CLS) [3] as eigenstates with strictly compact support. FB networks were extensively studied theoretically in $d = 1$ [4–6], $d = 2$ [7–9], and $d = 3$ [7,10–15] lattice dimensions. Models featuring FBs have been experimentally realized in a variety of settings, including optical wave guide networks [16–20], exciton-polariton condensates [21–24], and ultracold atomic condensates [18,19,21,25–30].

Due to their fine-tuned character, flat-band systems are fragile to perturbations that can easily destroy the macroscopic degeneracy. As a consequence, exotic phases of matter with unusual properties emerge under the effect of various perturbations: disorder [31–35], external fields [36–38], nonlinearities [39–41]. Interactions in FB lead to a plethora of interesting phenomena: delocalization and conserved quantities [42–45], disorder-free many-body localization [44,46–48], ground-state ferromagnetism [7,8,12,49–52], pair formation for hard core bosons [53], superfluidity [54–56], and superconductivity [57].

However, the very defining feature of the flat bands—their fine-tuned degeneracy—makes it difficult to identify them in the relevant Hamiltonian parameter space. A number of methods have been proposed to construct FB lattices: line graph approach [7], extended cell construction method [8], origami rules [58], repetitions of miniarrays [59], local symmetry partitioning [60], chiral symmetry [15], fine tuning relying on specific CLS and network symmetries [10,61], using specific properties of FB [62], etc. All these methods apply to either specific geometries of the underlying networks or to networks with particular symmetries.

All the above discussed FB networks support CLS. It follows that the properties of the CLS together with a number of generic network properties form a set of classifiers, which will fix a particular FB network class. That approach leads to systematic FB generators based on these classifiers. The CLS classifiers are its size U (of occupied unit cells) and shape (in dimensions $d \geqslant 2$), while the generic network classifiers are its dimension d, the Bravais lattice type, the hopping range, and the number of bands ν (i.e., the number of sites per unit cell). The simplest generator case $U = 1$ with arbitrary remaining network classifiers was obtained in Ref. [63]. The more sophisticated case $U = 2$ with $d = 1$, nearest neighbor unit cell hopping, and two bands $\nu = 2$ was solved in closed form in Ref. [64], with its extension to larger band number ν and CLS size U published in Ref. [65].

In this work, we extend the $d = 1$ FB generator [64,65] to two dimensions $d = 2$ and indicate the road to generators in dimension $d = 3$. We introduce a systematic classification of $d = 2$ FB networks using their CLS classifiers, size U and shape. We demonstrate how to find analytic solutions for some FB classes. We regenerate and classify some of the already known $d = 2$ FB lattices such as the checkerboard, kagome, Lieb, and Tasaki lattices, along with a multitude of completely new $d = 2$ FB lattices.

The paper is organized as follows. In Sec. II, we introduce the main definitions and conventions that we use throughout

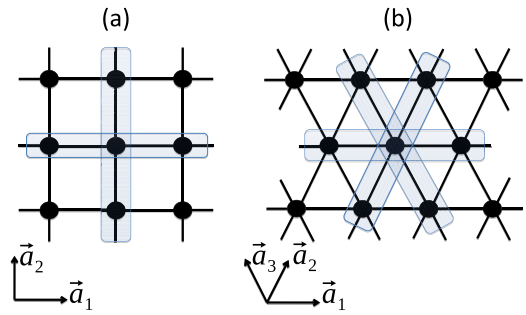

FIG. 1. Example of nearest neighbor unit cells for two-dimensional (2D) lattices, where $\vec{a}_1$, $\vec{a}_2$ are primitive translation vectors and $\vec{a}_3 = \vec{a}_1 + \vec{a}_2$. In our conventions: (a) a square lattice has only 2 nearest neighbor hopping directions: $\vec{a}_1$, $\vec{a}_2$, (b) a triangular/hexagonal lattice has 3 nearest neighbor hopping directions: $\vec{a}_{i=1,2,3}$.

the text. These conventions are direct generalization to $d = 2$ of the conventions used for the $d = 1$ FB generator [64,65]. Section II B introduces CLS of $d = 2$ FB Hamiltonians, and the classification of FB Hamiltonians by their CLS. It also presents an inverse eigenvalue problem for finding Hamiltonians from a given CLS class. An algorithm to solve these inverse eigenvalue problems is turned into an efficient FB generator in Sec. III B. In Sec. IV, we apply the FB generator to some classes of CLS, illustrate how the inverse eigenvalue problem is resolved and show the results. We conclude by summarizing our results and discussing open problems.

II. MAIN DEFINITIONS

A. Models

We consider a $d = 2$ translational invariant tight-binding lattice with ν sites per unit cell. We use the same notation as in our previous works, Refs. [64,65]: we label wave functions by the unit cell index n, so that the full wave function reads $\Psi = (\vec{\psi}_1, \ldots, \vec{\psi}_n, \ldots)$, where the ν-component vector $\vec{\psi}_n$ is the wave function of the nth unit cell. For simplicity we restrict to nonzero hopping between nearest neighbor unit cells only, and note that the generalization to longer-range hoppings is cumbersome but straightforward. Nearest neighbor unit cells are defined along (combinations of) primitive lattice translation vectors. A set of matrices H_χ describes the hopping between different pairs of unit cells. The index χ encodes the direction of the hopping, x, y, etc. The result is illustrated in Fig. 1 for a square lattice and a triangular lattice, the only possible cases for the nearest neighbor directions in $d = 2$. A unit cell on the square lattice has four neighbors and two different directions of nearest neighbor hopping, both along the primitive lattice translations vectors $\vec{a}_1$ and $\vec{a}_2$. A site on a triangular lattice has six neighbors and three possible directions of nearest neighbor hopping: $\vec{a}_{i=1,2,3}$ only two of which correspond to the primitive lattice translation vectors. With these conventions the Hamiltonian eigenvalue problem reads

$$H_0\vec{\psi}_n + \sum_\chi (H_\chi^\dagger \vec{\psi}_{n'_\chi} + H_\chi \vec{\psi}_{n_\chi}) = E\vec{\psi}_n, \quad n \in \mathbb{Z}. \tag{1}$$

Here H_0 describes the intracell hopping and H_χ is the nearest neighbor hopping matrix for the χth direction, with n_χ and n'_χ being the respective indices of the two nearest neighboring unit cells along the χth direction. Because of the translation invariance the Floquet-Bloch theorem applies and the eigenstates of Eq. (1) can be expressed as $\vec{\psi}_n = \vec{u}(\mathbf{k})e^{-i\mathbf{k}\cdot\vec{R}_n}$, where the Bloch polarization vector $\vec{u}(\mathbf{k})$ has ν components $u_\mu(\mathbf{k})$, $\mu = 1, \ldots, \nu$. Finally $\mathbf{k} = (k_x, k_y)$ is the wave vector, and $\vec{R}_n$ is the position of the nth unit cell. Then the eigenvalue problem (1) in momentum space reads

$$H_\mathbf{k}\vec{u}(\mathbf{k}) = E(\mathbf{k})\vec{u}(\mathbf{k}). \tag{2}$$

The eigenvalues $E(\mathbf{k})$ provide the band structure of the Hamiltonian $H_\mathbf{k}$.

B. Classification of compact localized states

In our previous work [65] we have shown that the size U of a CLS is the only CLS-related flat-band classifier in dimension $d = 1$ dimension. For $d = 2$ dimensions, size and shape of the CLS plaquette turn into relevant flat-band classifiers. The size of a CLS is given by two integers U_1 and U_2, which define its plaquette size along the two primitive lattice translation vectors $\vec{a}_1$, $\vec{a}_2$. The shape of a CLS plaquette is encoded by a $U_1 \times U_2$ matrix T with integer entries 0 or 1. The zero elements of the matrix T prescribe the locations of unit cells with zero wave-function amplitudes in the CLS plaquette. The number of all possible nontrivial matrices T is finite and can be sorted and counted using an integer $s \geqslant 0$. Therefore we arrive at the extended CLS flat-band classifier vector $\mathbf{U} = (U_1, U_2, s)$.

For $U_1 = 1$ or $U_2 = 1$ there is only one possible shape and we can shorten the classifier $\mathbf{U}$ to $(1, U_2)$ or $(U_1, 1)$. The other cases considered below correspond to $U_1 = U_2 = 2$, and we choose the integer s to count the number of zeros in the above matrix T:

$$s = 0 \ : \ T = \begin{pmatrix} 1 & 1 \\ 1 & 1 \end{pmatrix}, \tag{3}$$

$$s = 1 \ : \ T = \begin{pmatrix} 1 & 0 \\ 1 & 1 \end{pmatrix}, \tag{4}$$

$$s = 2 \ : \ T = \begin{pmatrix} 0 & 1 \\ 1 & 0 \end{pmatrix}. \tag{5}$$

The case $U = 1$ discussed in the introduction corresponds to $\mathbf{U} = (1, 1)$. The simplest nontrivial case in $d = 2$ is $\mathbf{U} = (2, 1)$ and will be discussed below. The next and less trivial set of cases in $d = 2$ is $\mathbf{U} = (2, 2, 0)$, $\mathbf{U} = (2, 2, 1)$, and $\mathbf{U} = (2, 2, 2)$. Figure 2 shows some of the known cases of 2D flat-band networks with their CLS plaquettes: Fig. 2(a) Lieb: $\mathbf{U} = (2, 2, 1)$; Fig. 2(b) checkerboard: $\mathbf{U} = (2, 2, 1)$; Fig. 2(c) kagome: $\mathbf{U} = (2, 2, 1)$; and Fig. 2(d) dice: $\mathbf{U} = (2, 2, 0)$.

We will show that these known flat-band networks are members of vast families of flat-band networks, each with a number of continuously tunable control parameters. For $U_1, U_2 \leqslant 2$ the wave functions $\vec{\psi}_n$ in Eq. (1) are nonzero for a maximum of four unit cells. We label these CLS components as $\vec{\psi}_{i=1,\ldots,4}$ as shown in Fig. 3(e). We will use the vector $\vec{\psi}_i$ and the bra-ket $|\psi_i\rangle$ notations interchangeably throughout the text.

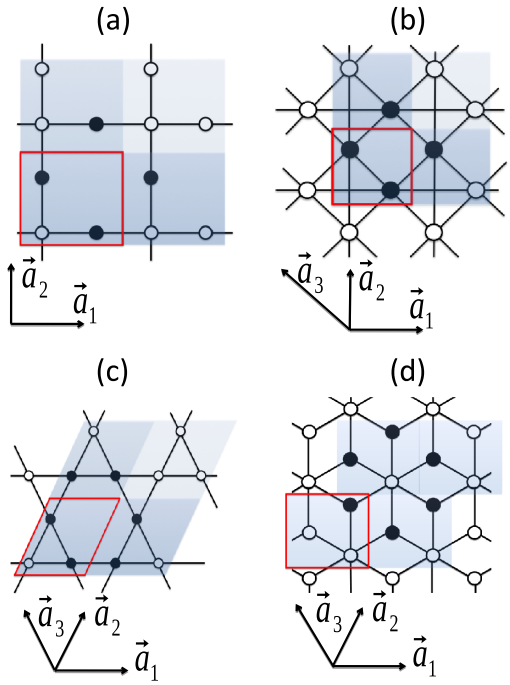

FIG. 2. The **U** classification of four specific and known 2D lattices with a flat band. Open circles denote the lattice sites, black lines nonzero hopping elements of equal value. Shaded areas indicate the $U_1 \times U_2$ CLS plaquette, and the darker shaded regions show the occupied unit cells (black circles show the nonzero wave function amplitudes of the flat-band CLS). Red boxes denote the unit cell, and $\vec{a}_1$, $\vec{a}_2$ are primitive translation vectors, and $\vec{a}_3 = \vec{a}_1 \pm \vec{a}_2$. Lattices and respective (extended) classifier vectors of the respective CLS: (a) Lieb: $\mathbf{U} = (2, 2, 1)$, (b) checkerboard: $\mathbf{U} = (2, 2, 1)$, (c) kagome: $\mathbf{U} = (2, 2, 1)$, and (d) dice: $\mathbf{U} = (2, 2, 0)$.

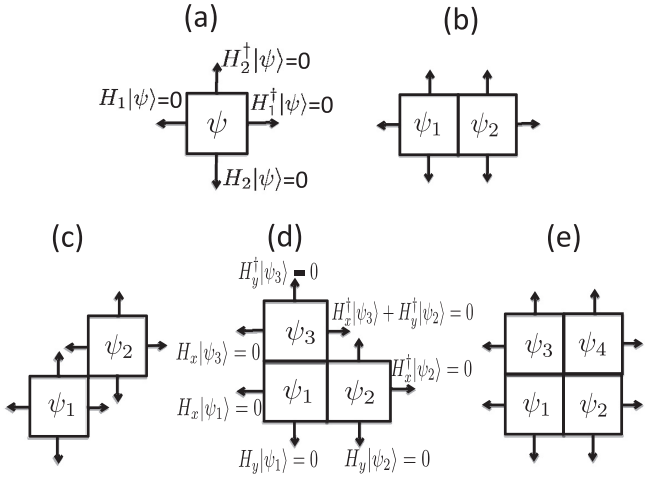

FIG. 3. Classification of compact localized states for cases with two hopping matrices. Each square represents a unit cell. Directions of the hopping and respective destructive interference conditions are indicated by arrows. Where two hopping terms (arrows) meet, both will contribute to the destructive interference cancellation. (a) $\mathbf{U} = (1, 1)$ single unit cell ($U = 1$) CLS. (b) $\mathbf{U} = (2, 1)$ case. (c) $\mathbf{U} = (2, 2, 2)$ case. (d) $\mathbf{U} = (2, 2, 1)$ case. (e) $\mathbf{U} = (2, 2, 0)$ case.

III. FLAT-BAND GENERATOR

A. Eigenvalue problem

Just as in the $d = 1$ case [65] we construct FB Hamiltonians from their CLS, considering the latter as input parameters and reformulating the problem of finding a FB Hamiltonian into an inverse eigenvalue problem for the hopping matrices H_χ. To achieve this we rewrite the eigenvalue problem (1) for the nonzero amplitudes $\vec{\psi}_i$ and supplement it with destructive interference conditions, which ensure the strict compactness of the eigenstate. Overall the way we solve this system in $d = 2$ is very similar in spirit to but is in general more complex and involved than the $d = 1$ case.

1. $U = 1$

The $U = 1$ case assumes a CLS, which occupies only one unit cell with wave function $\vec{\psi}_1$ and leads to a simple set of equations:

$$\begin{aligned} H_0\vec{\psi}_1 &= E_{\mathrm{FB}}\vec{\psi}_1, \\ H_i\vec{\psi}_1 &= H_i^\dagger\vec{\psi}_1 = 0, \quad i = 1, 2, 3. \end{aligned} \tag{6}$$

2. $U_1 = 2$

Two hopping matrices. The simplest case of two hopping matrices H_1, H_2 can be always related to a square lattice geometry. One example is the Lieb lattice shown in Fig. 2(a). The possible CLS shapes and the hoppings for this case are shown in Fig. 3. The eigenvalue problem and destructive interference conditions read:

$$\begin{aligned} H_1\vec{\psi}_2 + H_2\vec{\psi}_3\delta_{U_2,2} &= (E_{\mathrm{FB}} - H_0)\vec{\psi}_1, \\ H_1^\dagger\vec{\psi}_1 + H_2\vec{\psi}_4\delta_{U_2,2}\delta_{s,0} &= (E_{\mathrm{FB}} - H_0)\vec{\psi}_2, \\ (H_1\vec{\psi}_4\delta_{s,0} + H_2^\dagger\vec{\psi}_1)\delta_{U_2,2} &= (E_{\mathrm{FB}} - H_0)\vec{\psi}_3\delta_{U_2,2}, \\ (H_1^\dagger\vec{\psi}_3\delta_{s,0} + H_2^\dagger\vec{\psi}_2\delta_{s,0})\delta_{U_2,2} &= (E_{\mathrm{FB}} - H_0)\vec{\psi}_4\delta_{U_2,2}\delta_{s,0}, \\ H_1\vec{\psi}_1 = H_1^\dagger\vec{\psi}_2 &= 0, \\ H_2\vec{\psi}_1 = H_2\vec{\psi}_2 &= 0, \\ H_1\vec{\psi}_3\delta_{U_2,2} = H_2^\dagger\vec{\psi}_3\delta_{U_2,2} &= 0, \\ H_1\vec{\psi}_3\delta_{U_2,2}\delta_{s,1} + H_2^\dagger\vec{\psi}_2 &= 0, \\ H_1^\dagger\vec{\psi}_4\delta_{U_2,2}\delta_{s,0} = H_2^\dagger\vec{\psi}_4\delta_{U_2,2}\delta_{s,0} &= 0. \end{aligned} \tag{7}$$

For specific values of U_1, U_2 and s the above system gives the eigenvalue problem and destructive interference conditions for a CLS with the extended classifier vector $\mathbf{U} = (U_1, U_2, s)$.

Three hopping matrices. Several known flat-band lattice models have three hopping matrices, which connect different unit cells, for example checkerboard, kagome, and dice lattices [see Figs. 2(b)–2(d)]. The three respective hopping matrices H_1, H_2, H_3 are shown in Fig. 4. It is instructive to note that the freedom in choosing different unit cells has consequences in our classification scheme. As an example, the dice lattice with its unit cell choice in Fig. 2(d) falls into the category $\mathbf{U} = (2, 2, 0)$ with three nontrivial hopping matrices. The unit cell choice used in Fig. 1 in Ref. [37] leads to a much larger CLS plaquette with classifier $\mathbf{U} = (3, 3)$ (and three

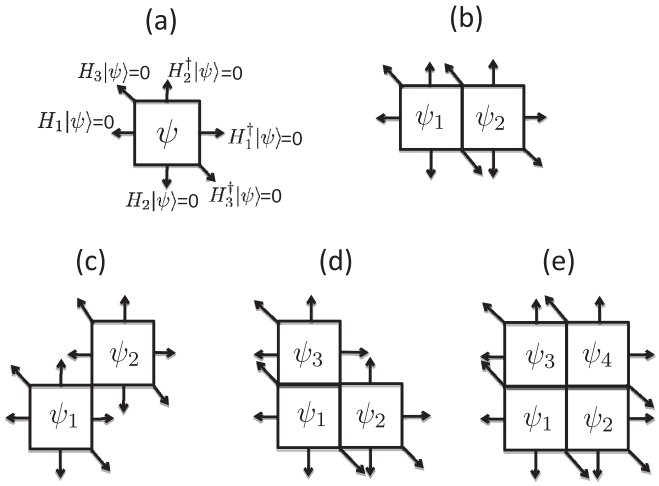

FIG. 4. Classification of compact localised states for cases with three hopping matrices. Each square represents a unit cell. Directions of the hopping and respective destructive interference conditions are indicated by arrows. Where two or more hopping terms (arrows) meet, all will contribute to the destructive interference cancellation. (a) $\mathbf{U} = (1, 1)$ single unit cell ($U = 1$) CLS. (b) $\mathbf{U} = (2, 1)$ case. (c) $\mathbf{U} = (2, 2, 2)$ case. (d) $\mathbf{U} = (2, 2, 1)$ case. (e) $\mathbf{U} = (2, 2, 0)$ case.

empty unit cells in the CLS), but also to a reduced number of only two nontrivial hopping matrices.

For three hopping matrices the eigenvalue problem and the corresponding destructive interference conditions read:

$$
\begin{aligned}
H_1\vec{\psi}_2 + H_2\vec{\psi}_3\delta_{U_2,2} &= (E_{\mathrm{FB}} - H_0)\vec{\psi}_1,\\
H_1^\dagger\vec{\psi}_1 + H_2\vec{\psi}_4\delta_{U_2,2}\delta_{s,0} + H_3^\dagger\vec{\psi}_3\delta_{U_2,2} &= (E_{\mathrm{FB}} - H_0)\vec{\psi}_2,\\
(H_1\vec{\psi}_4\delta_{s,0} + H_2^\dagger\vec{\psi}_1 + H_3\vec{\psi}_2)\delta_{U_2,2} &= (E_{\mathrm{FB}} - H_0)\vec{\psi}_3\delta_{U_2,2},\\
(H_1^\dagger\vec{\psi}_3 + H_2^\dagger\vec{\psi}_2)\delta_{U_2,2}\delta_{s,0} &= (E_{\mathrm{FB}} - H_0)\vec{\psi}_4\delta_{U_2,2}\delta_{s,0},\\
H_1\vec{\psi}_1 = H_2\vec{\psi}_1 &= 0,\\
H_1^\dagger\vec{\psi}_4\delta_{U_2,2}\delta_{s,0} = H_2\vec{\psi}_4\delta_{U_2,2}\delta_{s,0} &= 0,\\
H_3^\dagger\vec{\psi}_2 = H_3\vec{\psi}_3\delta_{U_2,2} &= 0,\\
H_2\vec{\psi}_2 + H_3^\dagger\vec{\psi}_1 &= 0,\\
H_1\vec{\psi}_3\delta_{U_2,2} + H_3\vec{\psi}_1\delta_{U_2,2} &= 0,\\
H_2^\dagger\vec{\psi}_3\delta_{U_2,2} + H_3\vec{\psi}_4\delta_{U_2,2}\delta_{s,0} &= 0,\\
H_1^\dagger\vec{\psi}_2 + H_3\vec{\psi}_4\delta_{U_2,2}\delta_{s,0} &= 0.
\end{aligned}
\tag{8}
$$

For specific values of U_1, U_2, s we obtain the eigenvalue problem and destructive interference conditions for a CLS with the extended classifier vector $\mathbf{U} = (U_1, U_2, s)$. In order to apply the generator defined below, we define the transverse projectors Q_i, Q_{ij}, Q_{ijk} on $\{\vec{\psi}_i\}$, $\{\vec{\psi}_i, \vec{\psi}_j\}$ and $\{\vec{\psi}_i, \vec{\psi}_j, \vec{\psi}_k\}$, respectively.

B. Generator

The sets of equations (7), (8) are the starting point of our flat-band generator. Our goal is to generate all possible matrices H_χ, which allow for the existence of a flat band, given a particular choice of the CLS shape, E_{FB} and H_0. We arrive at the following protocol:

(i) Choose the number of bands ν.
(ii) Choose a hopping range.
(iii) Choose a plaquette shape of the CLS.
(iv) Choose an arbitrary Hermitian H_0.
(v) Choose a flat-band energy E_{FB}.
(vi) Exclude H_1, H_2, and H_3 from the equations (7), (8) to get nonlinear constraints on the CLS components $\vec{\psi}_i$, and solve these constraints to find all CLS components $\vec{\psi}_i$.
(vii) With the chosen H_0, E_{FB} and the CLS $\vec{\psi}_i$ obtained at the previous step, solve equations (7), (8) for H_χ.

The above protocol admits variations, which can simplify the task. In some cases the nonlinear constraints allow us to skip item (v) and keep the flat-band energy E_{FB} a free parameter to be fixed when executing item (vi), as we will show below. Step (vi) requires solving nonlinear equations, which may have either no CLS solutions, or a manifold of CLS solutions with freely tunable parameters, or even several such manifolds. Using a CLS solution from step (vi), and executing step (vii), will in general yield a solution manifold of hopping matrices with freely tunable parameters as well, which correspond to the freedom of fixing only the flat-band states and not constraining the rest of the spectrum, bands, and eigenvectors.

IV. SOLUTIONS

We consider CLS sizes restricted to $U_1, U_2 \leqslant 2$, unless stated otherwise.

A. $U = 1$

Without loss of generality we assume that H_0 is diagonal with first diagonal entry E_{FB}. From the first line in Eq. (6) we conclude $\vec{\psi}_1 = (1, 0, 0, \ldots, 0)$. The following destructive interference conditions yield $(H_i)_{1,\mu} = (H_i)_{\mu,1} = 0$, i.e., the hopping matrices have zeros on their first row and column, and freely chooseable entries elsewhere. The entries parametrize the remaining dispersive degrees of freedom. These entries as well as an overall multiplicative scaling factor and energy gauge are the free parameters of the corresponding manifold of $U = 1$ flat-band Hamiltonians. These solutions correspond to the detangled basis of $U = 1$ flat-band networks [63]. Additional manifold parameters are obtained from entangling the CLS with the dispersive network through commuting local unitary operations [63].

For two bands $\nu = 2$ and $H_3 = 0$ it follows that the only solutions are either $U = 1$ flat bands, or decoupled 1D networks with $H_2 = 0$ and $U = 2$ (see details of the derivation in Appendix A).

B. U = (2, 1)

A schematic of the CLS and the destructive interference conditions for this case are shown in Fig. 3(b) and Fig. 4(b) for the two and three hopping matrices cases, respectively. The eigenvalue problem (7), respectively (8), involves only one hopping matrix H_1, while the matrices $H_{2,3}$ enter additional destructive interference conditions only. Therefore the eigen-

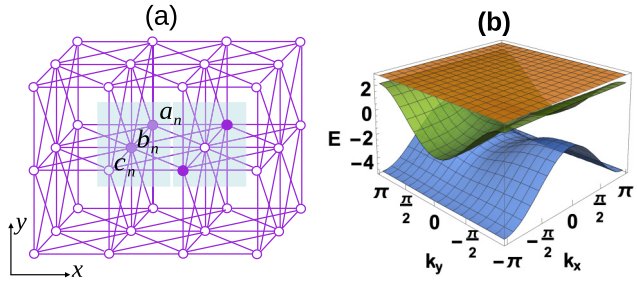

FIG. 5. Example of a $\mathbf{U} = (2, 1)$ CLS FB network and $\nu = 3$. (a) Tight binding lattice with two hopping matrices. Lines indicate nonzero hoppings, filled circles show the position of a CLS. a_n, b_n, c_n indicate the sites in one unit cell. See Appendix B1 for details. (b) Band structure corresponding to (a).

value problem reduces to the 1D case solved in Ref. [65]. It follows (see Appendix B1 and Ref. [65] for details)

$$H_1 = \frac{(E_{\rm FB} - H_0)|\psi_1\rangle\langle\psi_2|(E_{\rm FB} - H_0)}{\langle\psi_1|E_{\rm FB} - H_0|\psi_1\rangle}. \tag{9}$$

The CLS components $\vec{\psi}_1$, $\vec{\psi}_2$ are subject to nonlinear constraints

$$\begin{aligned}\langle\psi_2|E_{\rm FB} - H_0|\psi_1\rangle &= 0,\\ \langle\psi_1|E_{\rm FB} - H_0|\psi_1\rangle &= \langle\psi_2|E_{\rm FB} - H_0|\psi_2\rangle,\end{aligned} \tag{10}$$

that are resolved similarly to the 1D case [65]. For two hopping matrices the additional destructive interference yields

$$H_2 = Q_{12}M_2Q_{12}, \tag{11}$$

where M_2 is an arbitrary $\nu \times \nu$ matrix. Figure 5 provides an example network for the two hopping matrices case. For three hopping matrices the derivation of H_2 and H_3 is given in Appendix C1.

C. U = (2, 2, 2)

The case $\mathbf{U} = (2, 2, 2)$ is shown in Figs. 3(c) and 4(c), where the two CLS-occupied unit cells just touch one another. Equations (7)–(8) reduce to simple eigenproblems for the amplitudes in each individual unit cell:

$$H_0|\psi_{i=1,2}\rangle = E_{\rm FB}|\psi_{i=1,2}\rangle. \tag{12}$$

We choose some H_0 and thereby fix $E_{\rm FB}$ and $\vec{\psi}_{1,2}$. If $E_{\rm FB}$ is nondegenerate, then $\vec{\psi}_2 \propto \vec{\psi}_1$ and the problem reduces to a $U = 1$ CLS. If $E_{\rm FB}$ is degenerate we need at least $\nu = 3$ bands. The amplitudes $\vec{\psi}_{1,2}$ can then be picked as distinct linear combinations of the eigenvectors corresponding to $E_{\rm FB}$. The intracell hopping matrices H_1, H_2, H_3 are reconstructed from the destructive interference conditions, Eqs. (7)–(8):

$$\begin{aligned} H_1|\psi_1\rangle = H_2|\psi_1\rangle = 0 \qquad & \langle\psi_2|H_1 = \langle\psi_2|H_2 = 0\\ H_1^\dagger|\psi_1\rangle + H_2|\psi_2\rangle = 0 \qquad & H_2^\dagger|\psi_1\rangle + H_1|\psi_2\rangle = 0\\ H_3|\psi_1\rangle = H_3^\dagger|\psi_1\rangle = H_3|\psi_2\rangle = H_3^\dagger|\psi_2\rangle &= 0.\end{aligned}$$

The last line implies that $H_3 = Q_{12}MQ_{12}$ where M is an arbitrary $\nu \times \nu$ matrix. The first two lines of the above equation constitute a coupled inverse problem of finding H_1, H_2 from their known action on $\vec{\psi}_1$, $\vec{\psi}_2$. This problem can be decoupled into inverse problems for H_1 and H_2 by defining:

$$H_1|\psi_1\rangle = Q_1|z\rangle \qquad H_1|\psi_2\rangle = Q_2|w\rangle. \tag{13}$$

The inverse problems for H_1, H_2 have been solved in Ref. [65].

D. U = (2, 2, 1)

A schematic of the CLS and destructive interference conditions for this case is shown in Fig. 3(d) and Fig. 4(d) for the two and three hopping matrices, respectively.

1. Two hopping matrices

The case of two hopping matrices and an arbitrary number of bands can be resolved following a similar derivation as for $\mathbf{U} = (2, 1)$, however, the solution is cumbersome. Therefore for simplicity we focus on the specific case of $\nu = 3$ bands. We can consider two cases: (a) the CLS amplitudes are linearly independent, or (b) the CLS amplitudes are dependent. The latter case includes the known cases of the Lieb [11] and Tasaki [8,49] lattices.

Case (a) has one of the destructive interference conditions reading $\langle\psi_3|H_1 + \langle\psi_2|H_2 = 0$. For $\nu = 3$ the number of components of each of the vectors $\Psi_{1,2,3}$ is also equal to three. Therefore it is straightforward to show that the destructive interference condition splits into two:

$$\langle\psi_3|H_1 = \langle\psi_2|H_2 = 0. \tag{14}$$

Then the eigenvalue problem Eq. (7) reads

$$\begin{aligned} H_1\vec{\psi}_2 + H_2\vec{\psi}_3 &= (E_{\rm FB} - H_0)\vec{\psi}_1,\\ H_1^\dagger\vec{\psi}_2 &= (E_{\rm FB} - H_0)\vec{\psi}_2,\\ H_2^\dagger\vec{\psi}_2 &= (E_{\rm FB} - H_0)\vec{\psi}_3,\\ H_1\vec{\psi}_2 = H_1^\dagger\vec{\psi}_2 = H_1\vec{\psi}_3 &= H_1^\dagger\vec{\psi}_3 = 0,\\ H_2\vec{\psi}_2 = H_2^\dagger\vec{\psi}_3 = H_2\vec{\psi}_2 &= H_2^\dagger\vec{\psi}_2 = 0.\end{aligned} \tag{15}$$

We eliminate H_1, H_2 from the eigenproblem and obtain the nonlinear constraints on the CLS amplitudes:

$$\begin{aligned} \langle\psi_2|H_0|\psi_1\rangle &= E_{\rm FB}\langle\psi_2||\psi_1\rangle,\\ \langle\psi_3|H_0|\psi_1\rangle &= E_{\rm FB}\langle\psi_3||\psi_1\rangle,\\ \langle\psi_3|H_0|\psi_2\rangle &= E_{\rm FB}\langle\psi_3||\psi_2\rangle,\\ &\quad\times\langle\psi_2|E_{\rm FB} - H_0|\psi_2\rangle\\ &\quad+\langle\psi_3|E_{\rm FB} - H_0|\psi_3\rangle\\ &= \langle\psi_1|E_{\rm FB} - H_0|\psi_1\rangle.\end{aligned} \tag{16}$$

Finally we obtain the hopping matrices:

$$\begin{aligned} H_1 &= \frac{(E_{\rm FB} - H_0)|\psi_1\rangle\langle\psi_2|(E_{\rm FB} - H_0)}{\langle\psi_1|E_{\rm FB} - H_0|\psi_1\rangle},\\ H_2 &= \frac{(E_{\rm FB} - H_0)|\psi_1\rangle\langle\psi_3|(E_{\rm FB} - H_0)}{\langle\psi_1|E_{\rm FB} - H_0|\psi_1\rangle}.\end{aligned} \tag{17}$$

Case (b) assumes $\vec{\psi}_{i=1,2,3}$ to be linearly dependent

$$|\psi_1\rangle = \alpha|\psi_2\rangle + \beta|\psi_3\rangle. \tag{18}$$

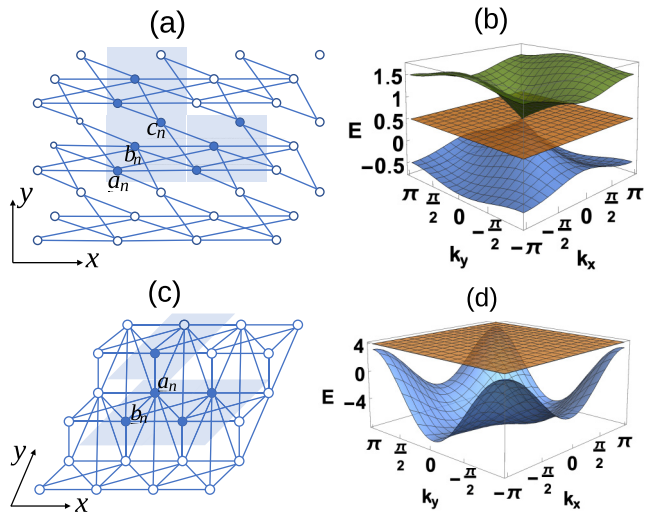

FIG. 6. Examples of $\mathbf{U} = (2, 2, 1)$ CLS FB networks. (a) Tight binding lattice with two hopping matrices and $\nu = 3$. Lines indicate nonzero hoppings, filled circles show the position of a CLS. a_n, b_n, c_n indicate the sites in one unit cell. See Appendix B2 for details. (b) Band structure corresponding to (a). (c) Same as (a) but for three hopping matrices and $\nu = 2$. a_n, b_n indicate the sites in one unit cell. See Appendix C2 for details. (d) Band structure corresponding to (c).

This yields the following solution (see details in Appendix B2):

$$H_1 = \frac{Q_2|a\rangle\langle\psi_2|(E_{\rm FB} - H_0)}{\langle\psi_3|Q_2|a\rangle},$$
$$H_2 = \frac{Q_3|b\rangle\langle\psi_3|(E_{\rm FB} - H_0)}{\langle\psi_2|Q_3|b\rangle}, \tag{19}$$

where $|a\rangle$, $|b\rangle$ are arbitrary vectors, and $E_{\rm FB}$, H_0, $\vec{\psi}_2$, $\vec{\psi}_3$ are chosen respecting the constraints

$$\langle\psi_2|E_{\rm FB} - H_0|\psi_2\rangle = 0,$$
$$\langle\psi_3|E_{\rm FB} - H_0|\psi_3\rangle = 0,$$
$$\langle\psi_3|E_{\rm FB} - H_0|\psi_2\rangle = 0,$$
$$(E_{\rm FB} - H_0)(\alpha|\psi_2\rangle + \beta|\psi_3\rangle) = 0. \tag{20}$$

Equations (18)–(20) provide a complete solution to this special $\mathbf{U} = (2, 2, 1)$ case with $\nu = 3$ bands. The known examples such as Lieb lattice and Tasaki's lattice can be constructed from our generator as demonstrated in Appendix B2. Figure 6(a), 6(b) shows one generated example (see details in Appendix B2).

2. Three hopping matrices

The configuration of this case is shown in Fig. 4(d). The eigenvalue problem and the destructive interference conditions read

$$H_1|\psi_2\rangle + H_2|\psi_3\rangle = (E_{\rm FB} - H_0)|\psi_1\rangle,$$
$$H_1^\dagger|\psi_1\rangle + H_3^\dagger|\psi_3\rangle = (E_{\rm FB} - H_0)|\psi_2\rangle,$$
$$H_2^\dagger|\psi_1\rangle + H_3|\psi_2\rangle = (E_{\rm FB} - H_0)|\psi_3\rangle,$$
$$H_1|\psi_1\rangle = H_2|\psi_1\rangle = H_3|\psi_3\rangle = 0,$$

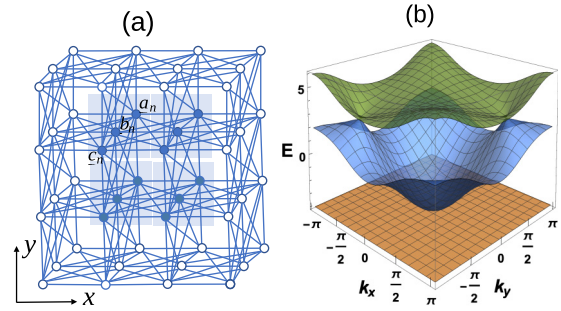

FIG. 7. Example of a $\mathbf{U} = (2, 2, 0)$ CLS FB network, two hopping matrices, and $\nu = 3$. (a) Tight-binding lattice. Lines indicate nonzero hoppings, filled circles show the position of a CLS. a_n, b_n, c_n indicate the sites in one unit cell. See Appendix B3 for details. (b) Band structure corresponding to (a).

$$\langle\psi_2|H_1 = \langle\psi_3|H_2 = \langle\psi_2|H_3 = 0,$$
$$H_1|\psi_3\rangle + H_3|\psi_1\rangle = 0,$$
$$H_2|\psi_2\rangle + H_3^\dagger|\psi_1\rangle = 0,$$
$$\langle\psi_3|H_1 + \langle\psi_2|H_2 = 0. \tag{21}$$

The family of flat-band solutions for two bands $\nu = 2$ is derived in Appendix C2, with a particular member choice of the family shown in Figs. 6(c), 6(d). Notably the checkerboard lattice [7,12,66,67] is also part of the family, as outlined in Appendix C2. For $\nu = 3$ a more cumbersome derivation yields the family of flat-band solutions that contains the kagome lattice [13,68,69] (not shown here).

E. U = (2, 2, 0)

The CLS and destructive interference conditions for the case of two hopping matrices and the square shaped CLS are shown in Fig. 3(e). For simplicity we restrict ourselves to three bands and use a direct parametrization of the CLS amplitudes $\vec{\psi}_i$ to solve Eq. (7). The full analytical solution is reported in Appendix B3. There are three free parameters in this solution, and Fig. 7 shows an example FB Hamiltonian for this case.

To conclude we note that the increased complexity of the equations (7)–(8) for fully 2D shapes as compared to the 1D case is an expected and generic feature. However, while it does not seem to be possible to work out full solutions in general—the nonlinear constraints on the amplitudes and complex destructive interference conditions typically being the main obstacle—we believe that such solutions can be found in individual cases.

V. CONCLUSIONS

In this work, we extended the systematic 1D flat-band generator [65] to two dimensions. Two important additional classifiers have been identified and added to make the 2D generator complete. First, we need to specify the underlying Bravais lattice class. Second and most importantly we need to specify the shape of the compact localized states at otherwise fixed CLS plaquette size. We derived analytical solutions for a number of different FB classes, and reproduced some of the well-known FB lattices: Lieb, Tasaki, kagome, and

checkerboard, along with a number of new 2D FB lattice examples. Our generator results in the possibility of counting free continuously variable parameters after fixing one particular 2D FB class. These existing parameters demonstrate that FB Hamiltonians, while being fine-tuned models, emerge as members of finite-dimensional Hamiltonian manifolds with an additional rich structure. Our results can be straightforwardly extended to larger compact localized states in 2D, and also to 3D cases, no matter how cumbersome the derivations could turn. Therefore our FB generator provides a direct way to search for flat bands for fixed lattice geometries in any lattice dimension. In particular our generator might shed light on the origin and some properties of nearly flat-bands observed in twisted bilayer graphene [70]: several studies [71,72] suggest a proximity to a chiral lattice system with perfect flat bands at $E = 0$, whose properties require careful investigation. Another interesting direction is experimental realizations of flat-band lattices: while several well-known lattices with flat bands were observed experimentally—Lieb [19,20,24,25,73], kagome [16,21,74], honeycomb [22], super-honeycomb [75]—our generator with minimal modifications allows us to construct new flat-band lattices in experimentally relevant geometries.

ACKNOWLEDGMENT

This work was supported by the Institute for Basic Science in Korea (IBS-R024-D1).

APPENDIX A: $\nu = 2$ AND $H_3 = 0$

We consider two bands and $H_3 = 0$ and demonstrate that any possible flat bands always either reduce to class $U = 1$ or decouple into 1D networks. First we consider the $\mathbf{U} = (2, 1)$ case in Fig. 3(b). The eigenvalue problem and the destructive interference conditions (7) read

$$\begin{aligned} H_0\vec{\psi}_1 + H_1\vec{\psi}_2 &= E_{\mathrm{FB}}\vec{\psi}_1, \\ H_0\vec{\psi}_2 + H_1^\dagger\vec{\psi}_1 &= E_{\mathrm{FB}}\vec{\psi}_2, \\ H_1\vec{\psi}_1 = H_1^\dagger\vec{\psi}_2 &= 0, \\ H_2\vec{\psi}_s = H_2^\dagger\vec{\psi}_s &= 0, \quad s = 1, 2. \end{aligned} \tag{A1}$$

The last line enforces that either (i) $H_2 = 0$ or (ii) $\vec{\psi}_2 \propto \vec{\psi}_1$. Case (i) reduces the system to a set of disconnected 1D networks, which were completely studied in Ref. [64]. Case (ii) yields that $\vec{\psi}_{1,2}$ are an eigenvector to H_0 (up to a normalization factor) and form a complete $U = 1$ CLS, and the considered $\mathbf{U} = (2, 1)$ case reduces to a linear combination of two $U = 1$ CLS states.

For the $\mathbf{U} = (2, 2, 0)$ case in Fig. 3(e) the destructive interference conditions in Eq. (7) read

$$\begin{aligned} H_1\vec{\psi}_1 = H_1\vec{\psi}_3 &= 0, \\ H_1^\dagger\vec{\psi}_2 = H_1^\dagger\vec{\psi}_4 &= 0, \\ H_2\vec{\psi}_1 = H_2\vec{\psi}_2 &= 0, \\ H_2^\dagger\vec{\psi}_3 = H_2^\dagger\vec{\psi}_4 &= 0. \end{aligned} \tag{A2}$$

The first line enforces that either (i) $H_1 = 0$ or (ii) $\vec{\psi}_3 \propto \vec{\psi}_1$. Case (i) reduces the system to disconnected 1D networks. The third line results in (iia) $H_2 = 0$ or (iib) $\vec{\psi}_2 \propto \vec{\psi}_1$. Case (iia) reduces the system to disconnected 1D networks. Case (iib) implies $\vec{\psi}_4 \propto \vec{\psi}_1$ and reduces the problem to $U = 1$.

The case $\mathbf{U} = (2, 2, 1)$ shown in Fig. 3(d) yields the following destructive interference conditions:

$$\begin{aligned} H_1\vec{\psi}_1 = H_1\vec{\psi}_3 &= 0, \\ H_1^\dagger\vec{\psi}_2 &= 0, \\ H_2\vec{\psi}_1 = H_2\vec{\psi}_2 &= 0, \\ H_2^\dagger\vec{\psi}_3 &= 0, \\ H_1^\dagger\vec{\psi}_3 + H_2^\dagger\vec{\psi}_2 &= 0. \end{aligned} \tag{A3}$$

The first line enforces that either (i) $H_1 = 0$ or (ii) $\vec{\psi}_3 \propto \vec{\psi}_1$. Case (i) reduces the system to disconnected 1D networks. The third line results in (iia) $H_2 = 0$ or (iib) $\vec{\psi}_2 \propto \vec{\psi}_1$. Case (iia) reduces the system to disconnected 1D networks. Case (iib) reduces the problem to $U = 1$.

The case $\mathbf{U} = (2, 2, 2)$ shown in Fig. 3(c) is slightly more involved. The eigenproblem in this case reads:

$$H_0\vec{\psi}_{1,2} = E_{\mathrm{FB}}\vec{\psi}_{1,2}.$$

There are two possible solutions: (i) $\psi_2 \propto \psi_1$ or (ii) $H_0 = E_{\mathrm{FB}}\mathbb{I}$ and $\vec{\psi}_2 \perp \vec{\psi}_1$. Case (i) reduces the system to $U = 1$. In case (ii) we consider the destructive interference conditions

$$\begin{aligned} H_1\vec{\psi}_1 = H_2\vec{\psi}_1 &= 0 \\ H_1^\dagger\vec{\psi}_2 = H_2^\dagger\vec{\psi}_2 &= 0 \\ H_1\vec{\psi}_2 + H_2^\dagger\vec{\psi}_1 &= 0 \\ H_2\vec{\psi}_2 + H_1^\dagger\vec{\psi}_1 &= 0. \end{aligned}$$

From the first two lines and orthogonality of $\vec{\psi}_{1,2}$ we conclude that $H_{1,2} \propto |\psi_1\rangle\langle\psi_2|$. However, this is incompatible with the remaining two destructive interference conditions as verified by direct substitution and taking into account the mutual orthogonality of $\vec{\psi}_{1,2}$.

APPENDIX B: FB GENERATION FOR TWO HOPPING MATRICES AND $\nu \geqslant 3$

1. $U = (2, 1)$

From Eq. (7), we get the eigenvalue problem and destructive interference conditions

$$\begin{aligned} H_1|\psi_2\rangle &= (E_{\mathrm{FB}} - H_0)|\psi_1\rangle, \\ \langle\psi_1|H_1 &= \langle\psi_1|(E_{\mathrm{FB}} - H_0), \\ H_1|\psi_1\rangle = H_2|\psi_1\rangle &= H_2|\psi_2\rangle = 0, \\ \langle\psi_2|H_1 = \langle\psi_1|H_2 &= \langle\psi_2|H_2 = 0. \end{aligned} \tag{B1}$$

Since H_2 only appears in the destructive interference conditions, we can express it as $H_2 = Q_{12}M_2Q_{12}$ where M_2 is an arbitrary $\nu \times \nu$ matrix. The remaining problem is identical to the 1D problem discussed in our previous work [65] so that we only sketch the solution. Using the destructing interference

conditions, we eliminate H_1 from the eigenvalue problem and find the following nonlinear constraints on the CLS

$$\begin{aligned}&\langle\psi_2|E_{\rm FB}-H_0|\psi_1\rangle=0,\\&\langle\psi_1|E_{\rm FB}-H_0|\psi_1\rangle=\langle\psi_2|E_{\rm FB}-H_0|\psi_2\rangle.\end{aligned}\tag{B2}$$

The destructive interference conditions suggest the following ansatz $H_1=Q_2|u\rangle\langle v|Q_1$, where $|u\rangle$, $|v\rangle$ are vectors to be fixed. Plugging this ansatz into Eq. (B1) we find the vectors $\vec{u}$, $\vec{v}$ and the final expression for H_1

$$H_1=\frac{(E_{\rm FB}-H_0)|\psi_1\rangle\langle\psi_2|(E_{\rm FB}-H_0)}{\langle\psi_1|E_{\rm FB}-H_0|\psi_1\rangle}.\tag{B3}$$

a. $v=3$ example

We choose H_0 and we parameterize the CLS amplitudes and H_2 as follows:

$$\begin{aligned}&H_0=\begin{pmatrix}0&1&0\\1&0&1\\0&1&0\end{pmatrix},\ \vec{\psi}_1=\begin{pmatrix}a\\b\\c\end{pmatrix},\ \vec{\psi}_2=\begin{pmatrix}d\\e\\f\end{pmatrix},\\&H_2=Q_{12}|u\rangle\langle v|Q_{12},\\&\vec{u}=(u_1,u_2,u_3),\quad \vec{v}=(v_1,v_2,v_3).\end{aligned}$$

The nonlinear constraints (B2) yield $b=-\sqrt{2}f$, $d=f$, $c=e=0$. Then it follows that

$$H_1=\begin{pmatrix}-\frac{1}{\sqrt{2}}&-\frac{a}{2f}&-\frac{1}{\sqrt{2}}\\ \frac{2f}{a}-\frac{a}{2f}&\frac{4-\frac{a^2}{f^2}}{2\sqrt{2}}&\frac{2f}{a}-\frac{a}{2f}\\ \frac{1}{\sqrt{2}}&\frac{a}{2f}&\frac{1}{\sqrt{2}}\end{pmatrix},$$

$$H_2=\begin{pmatrix}\sqrt{2}Af^2&aAf&-\sqrt{2}Af^2\\ aAf&\frac{a^2A}{\sqrt{2}}&-aAf\\ -\sqrt{2}Af^2&-aAf&\sqrt{2}Af^2\end{pmatrix},$$

where

$$A=\frac{\left(\sqrt{2}au_2+2f(u_1-u_3)\right)[av_2+2f(v_1-v_3)]}{(a^2+4f^2)^2}.$$

The FB energy $E_{\rm FB}$ is then obtained from the first nonlinear constraint (B2).

The specific lattice structure of the Hamiltonian in Fig. 5(a) corresponds to the following choices of free parameter:

$$\begin{aligned}&x_3=x_1,y_3=y_1,x_2=1,y_2=5,u_3=u_1,\\&v_3=v_1,u_2=1,v_2=-5,f=-1,a=1.\end{aligned}$$

The hopping matrices and CLS amplitudes read

$$H_1=\begin{pmatrix}-\frac{1}{\sqrt{2}}&\frac{1}{2}&-\frac{1}{\sqrt{2}}\\ -\frac{3}{2}&\frac{3}{2\sqrt{2}}&-\frac{3}{2}\\ \frac{1}{\sqrt{2}}&-\frac{1}{2}&\frac{1}{\sqrt{2}}\end{pmatrix},$$

$$H_2=\begin{pmatrix}-\frac{2}{5}&\frac{\sqrt{2}}{5}&\frac{2}{5}\\ \frac{\sqrt{2}}{5}&-\frac{1}{5}&-\frac{\sqrt{2}}{5}\\ \frac{2}{5}&-\frac{\sqrt{2}}{5}&-\frac{2}{5}\end{pmatrix},$$

$$\vec{\psi}_1=\begin{pmatrix}1\\\sqrt{2}\\0\end{pmatrix},\quad \vec{\psi}_2=\begin{pmatrix}-1\\0\\-1\end{pmatrix}.$$

2. $U=(2,2,1)$ case and $v=3$

The eigenvalue problem and destructive interference conditions in Eq. (7) become

$$\begin{aligned}H_1\vec{\psi}_2+H_2\vec{\psi}_3&=(E_{\rm FB}-H_0)\vec{\psi}_2,\\H_1^\dagger\vec{\psi}_1&=(E_{\rm FB}-H_0)\vec{\psi}_2,\\H_2^\dagger\vec{\psi}_1&=(E_{\rm FB}-H_0)\vec{\psi}_3,\\H_1\vec{\psi}_1=H_1^\dagger\vec{\psi}_2&=H_1\vec{\psi}_3=0,\\H_2\vec{\psi}_1=H_2\vec{\psi}_2&=H_2^\dagger\vec{\psi}_3=0,\\H_1^\dagger\vec{\psi}_3+H_2^\dagger\vec{\psi}_2&=0.\end{aligned}\tag{B4}$$

Using the destructive interference conditions, we eliminate H_1, H_2 from the eigenproblem and obtain the nonlinear constraints on the CLS amplitudes:

$$\begin{aligned}\langle\psi_2|H_0|\psi_1\rangle&=E_{\rm FB}\langle\psi_2||\psi_1\rangle,\\\langle\psi_3|H_0|\psi_1\rangle&=E_{\rm FB}\langle\psi_3||\psi_1\rangle,\\\langle\psi_3|H_0|\psi_2\rangle&=E_{\rm FB}\langle\psi_3||\psi_2\rangle,\\&\times\langle\psi_2|E_{\rm FB}-H_0|\psi_2\rangle\\&+\langle\psi_3|E_{\rm FB}-H_0|\psi_3\rangle\\&=\langle\psi_1|E_{\rm FB}-H_0|\psi_1\rangle.\end{aligned}\tag{B5}$$

a. Linearly independent CLS components

In this case, as explained in the main text, the destructive interference condition involving both H_1 and H_2 decouples into two separate conditions. Then the eigenvalue problem Eq. (B4) reads

$$\begin{aligned}H_1\vec{\psi}_2+H_2\vec{\psi}_3&=(E_{\rm FB}-H_0)\vec{\psi}_1,\\H_1^\dagger\vec{\psi}_2&=(E_{\rm FB}-H_0)\vec{\psi}_2,\\H_2^\dagger\vec{\psi}_2&=(E_{\rm FB}-H_0)\vec{\psi}_3,\\H_1\vec{\psi}_2=H_1^\dagger\vec{\psi}_2&=H_1\vec{\psi}_3=H_1^\dagger\vec{\psi}_3=0,\\H_2\vec{\psi}_2=H_2^\dagger\vec{\psi}_3&=H_2\vec{\psi}_2=H_2^\dagger\vec{\psi}_2=0.\end{aligned}\tag{B6}$$

The nonlinear constraints on the amplitudes of the CLS are given by the same Eq. (B5). Assuming that the nonlinear constraints are resolved, we provide below the solution to Eq. (B6). We use the following single projector choices $H_1=Q_{23}|x\rangle\langle y|Q_{13}$ and $H_2=Q_{23}|v\rangle\langle w|Q_{12}$, where the transverse projectors are enforced by the desctructive interference conditions. Plugging in these expression into the eigenproblem (B6) and using the nonlinear constraints we find the hopping matrices:

$$\begin{aligned}H_1&=\frac{(E_{\rm FB}-H_0)|\psi_1\rangle\langle\psi_2|(E_{\rm FB}-H_0)}{\langle\psi_1|E_{\rm FB}-H_0|\psi_1\rangle},\\H_2&=\frac{(E_{\rm FB}-H_0)|\psi_1\rangle\langle\psi_3|(E_{\rm FB}-H_0)}{\langle\psi_1|E_{\rm FB}-H_0|\psi_1\rangle}.\end{aligned}\tag{B7}$$

b. Linearly dependent CLS components

The linear dependence of the CLS amplitudes $\vec{\psi}_1$, $\vec{\psi}_2$, $\vec{\psi}_3$ reads

$$|\psi_1\rangle=\alpha|\psi_2\rangle+\beta|\psi_3\rangle.\tag{B8}$$

This CLS is not necessarily reducible to the $U = 1$ class as long as the amplitudes are not all mutually proportional: For example, the Lieb lattice falls under the $U = (2, 2, 1)$ case and has $\vec{\psi}_1 = \vec{\psi}_2 + \vec{\psi}_3$. The constraints on the CLS (B5) in this case become

$$\begin{aligned}\langle\psi_2|E_{\rm FB} - H_0|\psi_2\rangle &= 0,\\ \langle\psi_3|E_{\rm FB} - H_0|\psi_3\rangle &= 0,\\ \langle\psi_3|E_{\rm FB} - H_0|\psi_2\rangle &= 0,\\ (E_{\rm FB} - H_0)(\alpha|\psi_2\rangle + \beta|\psi_3\rangle) &= 0.\end{aligned} \tag{B9}$$

For the given $E_{\rm FB}$, H_0 and CLS amplitudes, satisfying the above constraints, the eigenvalue problem and destructive interference conditions (B4) become

$$\begin{aligned}\beta\langle\psi_3|H_1 &= \langle\psi_2|(E_{\rm FB} - H_0),\\ \alpha\langle\psi_2|H_2 &= \langle\psi_3|(E_{\rm FB} - H_0),\\ H_1|\psi_2\rangle &= H_1|\psi_3\rangle = 0,\\ H_2|\psi_2\rangle &= H_2|\psi_3\rangle = 0,\\ \langle\psi_2|H_1 &= 0,\\ \langle\psi_3|H_2 &= 0.\end{aligned} \tag{B10}$$

These are two decoupled inverse eigenvalue problems for H_1 and H_2 that we resolve in the same way as before [65]. The hopping matrices read

$$\begin{aligned}H_1 &= \frac{Q_2|u\rangle\langle\psi_2|(E_{\rm FB} - H_0)}{\langle\psi_3|Q_2|u\rangle},\\ H_2 &= \frac{Q_3|v\rangle\langle\psi_3|(E_{\rm FB} - H_0)}{\langle\psi_2|Q_3|v\rangle},\end{aligned} \tag{B11}$$

where $E_{\rm FB}$, H_0, $\vec{u} = (u_1, u_2, u_3)$, $\vec{v} = (v_1, v_2, v_3)$ are free parameters; $\vec{\psi}_1$, $\vec{\psi}_2$ are constrained by Eq. (B9) while $\vec{u}$ should not to be proportional to $\vec{\psi}_2$, and $\vec{v}$ should not be proportional to $\vec{\psi}_3$.

c. Three band examples for the linearly dependent case

We choose H_0 and parameterize the CLS amplitudes as follows:

$$H_0 = \begin{pmatrix}0 & 0 & 0\\ 0 & 1 & 0\\ 0 & 0 & \epsilon\end{pmatrix}, \quad \psi_2 = \begin{pmatrix}a\\ b\\ c\end{pmatrix}, \quad \psi_3 = \begin{pmatrix}e\\ f\\ g\end{pmatrix}. \tag{B12}$$

a. Tasaki and Lieb lattice families. Here we demonstrate how the Lieb lattice with a flat band at $E_{\rm FB} = 0$ enforced by the chiral symmetry, and the related Tasaki lattice are derived from our solution. The nonlinear constraints (B9) give

$$\psi_2 = \begin{pmatrix}a\\ c\sqrt{\epsilon}(\pm i)\\ c\end{pmatrix}, \psi_3 = \begin{pmatrix}e\\ g\sqrt{\epsilon}(\pm i)\\ g\end{pmatrix}.$$

To reproduce the Lieb lattice Hamiltonian the following unitary transformation is used:

$$H_0' = UH_0U^\dagger, \quad \psi_2' = U\psi_2, \quad \psi_3' = U\psi_3,$$

where

$$U = \begin{pmatrix}\cos(\theta)\cos(\varphi) & \cos(\theta)\sin(\varphi)\sin(\phi) - \sin(\theta)\cos(\phi) & \cos(\theta)\sin(\varphi)\cos(\phi) + \sin(\theta)\sin(\phi)\\ \sin(\theta)\cos(\varphi) & \sin(\theta)\sin(\varphi)\sin(\phi) + \cos(\theta)\cos(\phi) & \sin(\theta)\sin(\varphi)\cos(\phi) - \cos(\theta)\sin(\phi)\\ -\sin(\varphi) & \cos(\varphi)\sin(\phi) & \cos(\varphi)\cos(\phi)\end{pmatrix}.$$

The Lieb lattice is recovered for the following choices of parameters:

$$\begin{aligned}&b = i\frac{a\sqrt{\epsilon}}{\sqrt{2}}, \quad f = -\frac{ia\alpha\sqrt{\epsilon}}{\beta\sqrt{2}}, \quad g = -\frac{a\alpha}{\beta\sqrt{2}},\\ &c = \frac{a}{\sqrt{2}}, \quad e = a \;\; \theta = -\frac{\pi}{2}, \quad \phi = \frac{3\pi}{4},\\ &\varphi = -\frac{\pi}{4}, \quad \epsilon = -1, \quad c = \frac{a}{\sqrt{2}}, \quad \beta = \alpha.\end{aligned}$$

Then the CLS amplitudes are given by

$$\psi_2' = \begin{pmatrix}0\\ -\sqrt{2}a\\ 0\end{pmatrix}, \quad \psi_3' = \begin{pmatrix}0\\ 0\\ \sqrt{2}a\end{pmatrix}, \quad \psi_1' = \alpha\begin{pmatrix}0\\ -\sqrt{2}a\\ \sqrt{2}a\end{pmatrix}.$$

With the choice $\theta = -\frac{\pi}{2}, \phi = \frac{3\pi}{4}, \epsilon = -1$ it follows

$$H_0' = \begin{pmatrix}0 & \sin(\varphi) & \cos(\varphi)\\ \sin(\varphi) & 0 & 0\\ \cos(\varphi) & 0 & 0\end{pmatrix}.$$

The hopping matrices H_1', H_2' are given by Eq. (B11):

$$H_1' = \begin{pmatrix}-\frac{u_1\sin(\varphi)}{u_3\alpha} & 0 & 0\\ 0 & 0 & 0\\ -\frac{\sin(\varphi)}{\alpha} & 0 & 0\end{pmatrix}, \quad H_2' = \begin{pmatrix}\frac{v_1\cos(\varphi)}{v_2\alpha} & 0 & 0\\ \frac{\cos(\varphi)}{\alpha} & 0 & 0\\ 0 & 0 & 0\end{pmatrix}.$$

The above hopping matrices correspond to the family of Tasaki lattices [8]. For $u_1 = v_1 = 0$, we retrieve the hopping matrices of the Lieb lattice family.

b. Obtaining the example in Fig. 6(a), 6(b). We choose $E_{\rm FB} = \epsilon, \epsilon \neq 0, 1$ and find

$$a = -\frac{b\sqrt{-f^2(\epsilon - 1)}}{f\sqrt{\epsilon}}, \; e = -\frac{\sqrt{f^2 - f^2\epsilon}}{\sqrt{\epsilon}}, \; \beta = -\frac{\alpha b}{f}.$$

Then Eq. (B11) yields the following solution:

$$\psi_2 = \begin{pmatrix}-\frac{bD}{f\sqrt{\epsilon}}\\ b\\ c\end{pmatrix}, \quad \psi_3 = \begin{pmatrix}-\frac{D}{\sqrt{\epsilon}}\\ f\\ g\end{pmatrix}, \quad \psi_1 = \alpha\psi_2 + \beta\psi_3,$$

$$H_1 = \begin{pmatrix} \frac{bBD\epsilon}{Af} & -\frac{bB(\epsilon-1)\sqrt{\epsilon}}{A} & 0 \\ \frac{bCD\sqrt{\epsilon}}{Af} & \frac{bC(1-\epsilon)}{A} & 0 \\ \frac{b^2D\sqrt{\epsilon}}{\alpha cf^2-\alpha bfg} & \frac{b^2-b^2\epsilon}{\alpha cf-\alpha bg} & 0 \end{pmatrix},$$

$$H_2 = \begin{pmatrix} -\frac{DfG\epsilon}{F} & \frac{f^2G(\epsilon-1)\sqrt{\epsilon}}{F} & 0 \\ -\frac{DfH\sqrt{\epsilon}}{F} & -\frac{f^2H(1-\epsilon)}{F} & 0 \\ -\frac{Df\sqrt{\epsilon}}{\alpha cf-\alpha bg} & \frac{f^2(\epsilon-1)}{\alpha(cf-bg)} & 0 \end{pmatrix},$$

where

$$D = \sqrt{-f^2(\epsilon-1)},$$
$$A = \alpha(cf-bg)(bfu_3 + cDu_1\sqrt{\epsilon} - cfu_2\epsilon),$$
$$B = b^2(Du_2 + fu_1\sqrt{\epsilon}) + bcDu_3 + c^2fu_1\sqrt{\epsilon},$$
$$C = b^2(Du_1\sqrt{\epsilon} + fu_2(1-\epsilon)) - bcfu_3\epsilon + c^2fu_2\epsilon,$$
$$F = \alpha(cf-bg)(Dgv_1\sqrt{\epsilon} + f^2v_3 - fgv_2\epsilon),$$
$$G = Dfv_2 + g(Dv_3 + gv_1\sqrt{\epsilon}) + f^2v_1\sqrt{\epsilon},$$
$$H = Dfv_1\sqrt{\epsilon} + f^2(v_2 - v_2\epsilon) - fgv_3\epsilon + g^2v_2\epsilon.$$

We use the following parameter values:

$$u_1 = 0, u_2 = 0, u_3 = 2, \alpha = 1, \beta = 1, v_1 = 0, v_2 = 0,$$
$$v_3 = 1, a = 0, b = -1, g = 0, \epsilon = \tfrac{1}{2}, c = 2, f = -1,$$

finding the CLS and hopping matrices

$$\psi_2 = \begin{pmatrix} -1 \\ -1 \\ 2 \end{pmatrix}, \quad \psi_3 = \begin{pmatrix} -1 \\ -1 \\ 0 \end{pmatrix}, \quad \psi_1 = \begin{pmatrix} -2 \\ -2 \\ 2 \end{pmatrix},$$
$$H_0 = \begin{pmatrix} 0 & 0 & 0 \\ 0 & 1 & 0 \\ 0 & 0 & \frac{1}{2} \end{pmatrix}, H_1 = \begin{pmatrix} \frac{1}{4} & -\frac{1}{4} & 0 \\ \frac{1}{4} & -\frac{1}{4} & 0 \\ \frac{1}{4} & -\frac{1}{4} & 0 \end{pmatrix},$$
$$H_2 = \begin{pmatrix} 0 & 0 & 0 \\ 0 & 0 & 0 \\ -\frac{1}{4} & \frac{1}{4} & 0 \end{pmatrix}.$$

The lattice structure and band structure corresponding to the above hopping matrices is shown in Figs. 6(a), 6(b).

3. $U = (2, 2, 0)$ case with three bands

Putting the values $U_2 = 2$, $s = 0$ to Eq. (7), we find the following eigenvalue problem:

$$\begin{aligned} H_1\psi_{2,1} + H_2\psi_{1,2} &= (E_{\rm FB} - H_0)\psi_{1,1} \\ H_1^\dagger\psi_{1,1} + H_2\psi_{2,2} &= (E_{\rm FB} - H_0)\psi_{2,1}, \\ H_1\psi_{2,2} + H_2^\dagger\psi_{1,1} &= (E_{\rm FB} - H_0)\psi_{1,2}, \\ H_1^\dagger\psi_{1,2} + H_2^\dagger\psi_{2,1} &= (E_{\rm FB} - H_0)\psi_{2,2}, \end{aligned} \tag{B13}$$

and destructive interference conditions

$$\begin{aligned} H_1\psi_{1,1} = H_1\psi_{1,2} = H_2\psi_{1,1} = H_2\psi_{2,1} = 0, \\ H_1^\dagger\psi_{2,1} = H_1^\dagger\psi_{2,2} = H_2^\dagger\psi_{1,2} = H_2^\dagger\psi_{2,2} = 0. \end{aligned} \tag{B14}$$

We assume that H_1, H_2 have two zero modes and parametrize the hopping matrices H_1, H_2 in the following way:

$$H_1 = |x\rangle\langle y| = \begin{pmatrix} ad & ae & af \\ bd & be & bf \\ cd & ce & cf \end{pmatrix}, \tag{B15}$$
$$H_2 = |u\rangle\langle v| = \begin{pmatrix} gr & gs & gt \\ hr & hs & ht \\ lr & ls & lt \end{pmatrix}, \tag{B16}$$

where

$$|x\rangle = \begin{pmatrix} a \\ b \\ c \end{pmatrix}, |y\rangle = \begin{pmatrix} d \\ e \\ f \end{pmatrix}, |u\rangle = \begin{pmatrix} g \\ h \\ l \end{pmatrix}, |v\rangle = \begin{pmatrix} r \\ s \\ t \end{pmatrix}.$$

The zero more of H_1, H_2 are given by (the top two lines correspond to H_1, the bottom two to H_2; in every raw the first two elements are the right eigenvectors, while the last two are the left ones)

$$\begin{pmatrix} -f \\ 0 \\ d \end{pmatrix}, \begin{pmatrix} -e \\ d \\ 0 \end{pmatrix}, \begin{pmatrix} -c \\ 0 \\ a \end{pmatrix}, \begin{pmatrix} -b \\ a \\ 0 \end{pmatrix},$$
$$\begin{pmatrix} -t \\ 0 \\ r \end{pmatrix}, \begin{pmatrix} -s \\ r \\ 0 \end{pmatrix}, \begin{pmatrix} -l \\ 0 \\ g \end{pmatrix}, \begin{pmatrix} -h \\ g \\ 0 \end{pmatrix}.$$

Next we enforce the constraints on H_1, H_2 and the CLS amplitudes by the destructive interference conditions (B14). Since $\psi_{1,1}$ is the right zero eigenmode of both H_1 and H_2, it has to be perpendicular to both $\vec{y}$ and $\vec{v}$, or equivalently it is parallel to the cross product of $\vec{y}$ and $\vec{v}$ and also parallel to one of the right zero eigenvectors of H_1, H_2:

$$\vec{\psi}_{1,1} = \alpha(y \times v) \parallel \begin{pmatrix} -f \\ 0 \\ d \end{pmatrix} \parallel \begin{pmatrix} -t \\ 0 \\ r \end{pmatrix},$$

where we have introduced the proportionality factor α, that we set to 1 for convenience. Treating the other CLS amplitudes in the same way (and setting the proportionality factors to 1 as well) we arrive at the following set of constraints on the elements of the CLS amplitudes:

$$\begin{aligned} t = f, b = s, e = h, c = l, \\ d = r = a = g. \end{aligned} \tag{B17}$$

Then the expressions for all ψ reduce to the following equations:

$$\psi_1 = \begin{pmatrix} (-bf + ef)\alpha \\ 0 \\ (ab - ae)\alpha\} \end{pmatrix} = \alpha' \begin{pmatrix} -f \\ 0 \\ a \end{pmatrix},$$
$$\psi_2 = \begin{pmatrix} (-bc + bf)\beta \\ (ac - af)\beta \\ 0 \end{pmatrix} = \beta' \begin{pmatrix} -b \\ a \\ 0 \end{pmatrix},$$
$$\psi_3 = \begin{pmatrix} (ce - ef)\gamma \\ (-ac + af)\gamma \\ 0 \end{pmatrix} = \gamma' \begin{pmatrix} -e \\ a \\ 0 \end{pmatrix},$$
$$\psi_4 = \begin{pmatrix} (bc - ce)\eta \\ 0 \\ (-ab + ae)\eta \end{pmatrix} = \eta' \begin{pmatrix} -c \\ 0 \\ a \end{pmatrix}, \tag{B18}$$

where $\alpha', \beta', \gamma', \eta'$ are given by

$$\alpha' = (b-e)\alpha, \quad \beta' = (c-f)\beta,$$
$$\gamma' = -c\gamma + f\gamma, \quad \eta' = -b\eta + e\eta. \tag{B19}$$

We can set one of the prefactors to 1: we choose $\eta = 1$. Then Eq. (B18) becomes

$$\psi_1 = \begin{pmatrix} -(b-e)f\alpha \\ 0 \\ a(b-e)\alpha \end{pmatrix}, \psi_2 = \begin{pmatrix} -b(c-f)\beta \\ a(c-f)\beta \\ 0 \end{pmatrix},$$
$$\psi_3 = \begin{pmatrix} -e(-c\gamma + f\gamma) \\ a(-c\gamma + f\gamma) \\ 0 \end{pmatrix}, \psi_4 = \begin{pmatrix} -c(-b+e) \\ 0 \\ a(-b+e) \end{pmatrix}.$$

We choose H_0 as

$$H_0 = \begin{pmatrix} 0 & 0 & 0 \\ 0 & 1 & 0 \\ 0 & 0 & \epsilon \end{pmatrix}.$$

Putting Eqs. (B17) and (B19) into Eq. (B16), we get the hopping matrices

$$H_1 = \begin{pmatrix} a^2 & ae & af \\ ab & be & bf \\ ac & ce & cf \end{pmatrix}, H_2 = \begin{pmatrix} a^2 & ab & af \\ ae & be & ef \\ ac & bc & cf \end{pmatrix}. \tag{B20}$$

The eigenvalue problem (B13) becomes

$$\begin{pmatrix} (b-e)(-a^2(c-f)(\beta+\gamma) + f\alpha E_{\rm FB}) \\ -a(b-e)(c-f)(b\beta + e\gamma) \\ a(b-e)(-c(c-f)(\beta+\gamma) + \alpha(\epsilon - E_{\rm FB})) \end{pmatrix} = 0,$$
$$\begin{pmatrix} (c-f)(a^2(b-e)(1+\alpha) + b\beta E_{\rm FB}) \\ a(c-f)((b-e)e(1+\alpha) + \beta - \beta E_{\rm FB}) \\ a(b-e)(c-f)(c+f\alpha) \end{pmatrix} = 0,$$
$$\begin{pmatrix} (c-f)(a^2(b-e)(1+\alpha) - e\gamma E_{\rm FB}) \\ a(c-f)(b(b-e)(1+\alpha) + \gamma(-1+E_{\rm FB})) \\ a(b-e)(c-f)(c+f\alpha) \end{pmatrix} = 0,$$
$$\begin{pmatrix} (b-e)(-a^2(c-f)(\beta+\gamma) - cE_{\rm FB}) \\ -a(b-e)(c-f)(b\beta + e\gamma) \\ a(b-e)(-(c-f)f(\beta+\gamma) - \epsilon + E_{\rm FB}) \end{pmatrix} = 0.$$

Assuming that $a \neq 0$, $c \neq f$, $b \neq e$ we solve the above equations (according to Eqs. (B18)–(B19) $a = 0$ makes the $\psi_{i=1,\ldots,4}$ proportional, i.e., we find $U = 1$ CLS; while $c \neq f$, $b \neq e$ enforces $\psi_{i=1,\ldots,4} = 0$). Setting $a = 1$ for convenience the solution is

$$b = \frac{\mathrm{sgn}(E_{\rm FB})\sqrt{2}(E_{\rm FB}-1)|1+\alpha|}{\sqrt{-\sqrt{-\alpha(1-E_{\rm FB})^2E_{\rm FB}^4\left(4(1+\alpha)^2 - \alpha E_{\rm FB}^2\right)} + (E_{\rm FB}-1)E_{\rm FB}\left(\alpha E_{\rm FB}^2 - 2(1+\alpha)^2\right)}},$$
$$c = \frac{\sqrt{\alpha(E_{\rm FB}-\epsilon}}{\sqrt{E_{\rm FB}}}, \quad f = -\frac{\sqrt{E_{\rm FB}-\epsilon}}{\sqrt{\alpha E_{\rm FB}}},$$
$$e = -\frac{|1+\alpha|^{-1}}{E_{\rm FB}\sqrt{2}}\sqrt{-\sqrt{-\alpha(E_{\rm FB}-1)^2E_{\rm FB}^4\left(4(1+\alpha)^2 - \alpha E_{\rm FB}^2\right)} + (E_{\rm FB}-1)E_{\rm FB}\left(\alpha E_{\rm FB}^2 - 2(1+\alpha)^2\right)},$$
$$\beta = \frac{-\alpha(E_{\rm FB}-1)E_{\rm FB}^3 + \sqrt{-\alpha(1-E_{\rm FB})^2E_{\rm FB}^4\left(4(1+\alpha)^2 - \alpha E_{\rm FB}^2\right)}}{2(1+\alpha)(E_{\rm FB}-1)E_{\rm FB}^2},$$
$$\gamma = -\frac{\alpha(E_{\rm FB}-1)E_{\rm FB}^3 + \ sqrt{-\alpha(E_{\rm FB}-1)^2E_{\rm FB}^4\left(4(1+\alpha)^2 - \alpha E_{\rm FB}^2\right)}}{2(1+\alpha)(E_{\rm FB}-1)E_{\rm FB}^2}.$$

Plugging these solutions into Eq. (B20) we get the following hopping matrices:

$$H_1 = \begin{pmatrix} 1 & -\frac{B}{\sqrt{2}} & -\frac{\sqrt{E_{\rm FB}-\epsilon}}{\sqrt{\alpha}\sqrt{E_{\rm FB}}} \\ \frac{\sqrt{2}(E_{\rm FB}-1)}{BE_{\rm FB}} & \frac{1}{E_{\rm FB}} - 1 & -\frac{\sqrt{2}(E_{\rm FB}-1)\sqrt{E_{\rm FB}-\epsilon}}{\sqrt{\alpha}BE_{\rm FB}^{3/2}} \\ \frac{\sqrt{\alpha}\sqrt{E_{\rm FB}-\epsilon}}{\sqrt{E_{\rm FB}}} & -\frac{\sqrt{\alpha}B\sqrt{E_{\rm FB}-\epsilon}}{\sqrt{2}\sqrt{E_{\rm FB}}} & \frac{\epsilon}{E_{\rm FB}} - 1 \end{pmatrix}, \quad H_2 = \begin{pmatrix} 1 & \frac{\sqrt{2}(E_{\rm FB}-1)}{BE_{\rm FB}} & -\frac{\sqrt{E_{\rm FB}-\epsilon}}{\sqrt{\alpha}\sqrt{E_{\rm FB}}} \\ -\frac{B}{\sqrt{2}} & \frac{1}{E_{\rm FB}} - 1 & \frac{B\sqrt{E_{\rm FB}-\epsilon}}{\sqrt{2}\sqrt{\alpha}\sqrt{E_{\rm FB}}} \\ \frac{\sqrt{\alpha}\sqrt{E_{\rm FB}-\epsilon}}{\sqrt{E_{\rm FB}}} & \frac{\sqrt{2}\sqrt{\alpha}(E_{\rm FB}-1)\sqrt{E_{\rm FB}-\epsilon}}{BE_{\rm FB}^{3/2}} & \frac{\epsilon}{E_{\rm FB}} - 1 \end{pmatrix},$$

where

$$A = \sqrt{-\alpha(E_{\rm FB}-1)^2E_{\rm FB}^4\left(4(\alpha+1)^2 - \alpha E_{\rm FB}^2\right)},$$
$$B = \sqrt{\frac{(E_{\rm FB}-1)E_{\rm FB}\left(\alpha E_{\rm FB}^2 - 2(\alpha+1)^2\right) - A}{(\alpha+1)^2E_{\rm FB}^2}}.$$

This solution has three free parameters $\epsilon, E_{\rm FB}, \alpha$. We choose the following values $\epsilon = -1, E_{\rm FB} = -4, \alpha = 1$ to generate the example shown in Fig. 7: $A = 0, B = \sqrt{5/2}$,

$$H_0 = \begin{pmatrix} 0 & 0 & 0 \\ 0 & 1 & 0 \\ 0 & 0 & -1 \end{pmatrix},$$

$$H_1 = \begin{pmatrix} 1 & -\frac{\sqrt{5}}{2} & -\frac{\sqrt{3}}{2} \\ \frac{\sqrt{5}}{2} & -\frac{5}{4} & -\frac{\sqrt{15}}{4} \\ \frac{\sqrt{3}}{2} & -\frac{\sqrt{15}}{4} & -\frac{3}{4} \end{pmatrix},$$

$$H_2 = \begin{pmatrix} 1 & \frac{\sqrt{5}}{2} & -\frac{\sqrt{3}}{2} \\ -\frac{\sqrt{5}}{2} & -\frac{5}{4} & \frac{\sqrt{15}}{4} \\ \frac{\sqrt{3}}{2} & \frac{\sqrt{15}}{4} & -\frac{3}{4} \end{pmatrix}.$$

APPENDIX C: FB GENERATION FOR THREE HOPPING MATRICES

1. $U = (2, 1)$

This case is shown in Fig. 4(b). The eigenvalue problem and destructive interference conditions for H_1 Eq. (8) are identical to the case of two hopping matrices and are solved in Appendix B1. The only difference are the destructive interference conditions for $H_{2,3}$:

$$\begin{aligned} H_2|\psi_1\rangle &= H_3|\psi_1\rangle = 0 \\ \langle\psi_2|H_2 &= \langle\psi_2|H_3 = 0, \\ H_2|\psi_2\rangle &+ H_3^\dagger|\psi_1\rangle = 0, \\ \langle\psi_1|H_2 &+ \langle\psi_2|H_3^\dagger = 0. \end{aligned} \tag{C1}$$

We define:

$$\begin{aligned} H_2 = Q_2M_2Q_3, \quad H_3 = Q_2M_3Q_1, \\ |x\rangle = Q_2|\psi_1\rangle, \quad |y\rangle = Q_1|\psi_2\rangle. \end{aligned}$$

Then the last two equations (C1) become:

$$\begin{aligned} Q_1M_3^\dagger Q_2|x\rangle = -Q_2M_2Q_1|y\rangle = -Q_{12}|a\rangle, \\ \langle y|Q_2M_3^\dagger Q_1 = -\langle x|Q_2M_2Q_1 = -Q_{12}\langle b|, \end{aligned}$$

where we have introduced two arbitrary vectors $\vec{a}$ and $\vec{b}$. For two bands $\nu = 2$ the above equations imply that the last two conditions in (C1) decouple, and therefore the problem reduces to $U = 1$ as in the case of two hopping matrices. For the number of bands $\nu > 2$ the problem of finding H_2 and H_3 reduces to two independent inverse eigenvalues problems: one for M_2 (H_2)

$$\begin{aligned} Q_2M_2Q_1|y\rangle = Q_{12}|a\rangle, \\ \langle x|Q_2M_2Q_1 = Q_{12}\langle b|, \end{aligned}$$

and a similar problem for the matrix M_3 (H_3). This is a linear problem: we search for a particular solution as

$$Q_2M_2Q_1 = |u\rangle\langle\overline{y}| + |\overline{x}\rangle\langle v|,$$

where we choose the overlined vectors so that: $\langle\overline{x}| \propto \langle x|$, $\langle\overline{x}||x\rangle = 1$, and $\langle\overline{y}| \propto \langle y|$, $\langle\overline{y}||y\rangle = 1$. We also assume that $\vec{u} \perp \vec{x}$ and $\vec{v} \perp \vec{y}$. We find upon substitution of the ansatz into the inverse problem:

$$Q_2|u\rangle = Q_{12}|a\rangle, \quad \langle v|Q_1 = \langle b|Q_{12}.$$

These $\vec{u}$ and $\vec{v}$ have the assumed previously orthogonality properties. It then follows that the full solution of (C1) for H_2 is given by:

$$H_2 = Q_{12}|a\rangle\langle\overline{y}|Q_1 + Q_2|\overline{x}\rangle\langle b|Q_{12} + Q_{12}K_2Q_{12}.$$

The inverse problem for H_3 is resolved the same way with minimal modifications.

2. $U = (2, 2, 1)$ and $\nu = 2$

We choose the following H_0 and parameterise the CLS amplitudes as follows:

$$H_0 = \begin{pmatrix} 0 & 1 \\ 1 & 0 \end{pmatrix}, \ \vec{\psi}_1 = \begin{pmatrix} p \\ r \end{pmatrix}, \ \vec{\psi}_2 = \begin{pmatrix} s \\ t \end{pmatrix}, \ \vec{\psi}_3 = \begin{pmatrix} u \\ v \end{pmatrix}.$$

We parametrize the hopping matrices and solve the eigenvalue problem and destructive interference conditions in Eq. (21):

$$H_1 = \begin{pmatrix} a & \frac{ac}{b} \\ b & c \end{pmatrix}, \ H_2 = \begin{pmatrix} d & e \\ \frac{df}{e} & f \end{pmatrix}, \ H_3 = \begin{pmatrix} g & \frac{gl}{h} \\ h & l \end{pmatrix}.$$

Then one of the possible solutions of the eigenvalue problem (21) reads

$$\begin{aligned} a &= \frac{r(bp-s)}{s^2}, \quad c = -\frac{bp}{r}, \\ d &= \frac{i\sqrt{b^2(p^2+s^2)(r^2-s^2) - 2bpr^2s + r^2s^2}}{s^2}, \quad f = 0, \\ g &= -\frac{i(bp-s)\sqrt{b^2(p^2+s^2)(r^2-s^2) - 2bpr^2s + r^2s^2}}{bs^3}, \\ l &= u = 0, \\ h &= -\frac{i\sqrt{b^2(p^2+s^2)(r^2-s^2) - 2bpr^2s + r^2s^2}}{rs}, \\ v &= -\frac{i\sqrt{b^2(p^2+s^2)(r^2-s^2) - 2bpr^2s + r^2s^2}}{bs}, \\ e &= -\frac{ip\sqrt{b^2(p^2+s^2)(r^2-s^2) - 2bpr^2s + r^2s^2}}{rs^2}, \\ t &= r\left(\frac{1}{b} - \frac{p}{s}\right), \quad E_{\mathrm{FB}} = \frac{b(p^2+s^2)}{rs}. \end{aligned}$$

The corresponding hopping matrices become

$$H_1 = \begin{pmatrix} \frac{r(bp-s)}{s^2} & -\frac{p(bp-s)}{s^2} \\ b & -\frac{bp}{r} \end{pmatrix},$$

$$H_2 = \begin{pmatrix} \frac{iA}{s^2} & -\frac{ipA}{rs^2} \\ 0 & 0 \end{pmatrix}, \ H_3 = \begin{pmatrix} -\frac{i(bp-s)A}{bs^3} & 0 \\ -\frac{iA}{rs} & 0 \end{pmatrix},$$

$$\vec{\psi}_1 = \begin{pmatrix} p \\ r \end{pmatrix}, \ \vec{\psi}_2 = \begin{pmatrix} s \\ r\left(\frac{1}{b} - \frac{p}{s}\right) \end{pmatrix}, \ \vec{\psi}_3 = \begin{pmatrix} 0 \\ -\frac{iA}{bs} \end{pmatrix},$$

where

$$A = \sqrt{b^2(p^2+s^2)(r^2-s^2) - 2bpr^2s + r^2s^2}.$$

The network shown in Figs. 6(c), 6(d) corresponds to the values $p = 1, r = 1, b = 2, s = 1$ and

$$H_1 = \begin{pmatrix} 1 & -1 \\ 2 & -2 \end{pmatrix}, \ H_1 = \begin{pmatrix} -\sqrt{3} & \sqrt{3} \\ 0 & 0 \end{pmatrix},$$

$$H_3 = \begin{pmatrix} \frac{\sqrt{3}}{2} & 0 \\ \sqrt{3} & 0 \end{pmatrix},$$

$$\psi_1 = \begin{pmatrix} 1 \\ 1 \end{pmatrix}, \ \psi_2 = \begin{pmatrix} 1 \\ -\frac{1}{2} \end{pmatrix}, \ \psi_3 = \begin{pmatrix} 0 \\ \frac{\sqrt{3}}{2} \end{pmatrix}.$$

It is straightforward to check that the well-known tight-binding checkerboard lattice is included in the above solution. We choose H_0 and the CLS amplitudes of the checkerboard model as input

$$H_0 = \begin{pmatrix} 0 & b \\ b & 0 \end{pmatrix}, \quad \psi_1 = \begin{pmatrix} a \\ -a \end{pmatrix}, \quad \psi_2 = \begin{pmatrix} a \\ 0 \end{pmatrix}, \quad \psi_3 = \begin{pmatrix} 0 \\ -a \end{pmatrix}.$$

The solution yields the checkerboard hopping matrices

$$H_1 = \begin{pmatrix} 0 & 0 \\ b & b \end{pmatrix}, \quad H_2 = \begin{pmatrix} b & b \\ 0 & 0 \end{pmatrix}, \quad H_3 = \begin{pmatrix} 0 & b \\ 0 & 0 \end{pmatrix}.$$

[1] O. Derzhko, J. Richter, and M. Maksymenko, Strongly correlated flat band systems: The route from heisenberg spins to hubbard electrons, Int. J. Mod. Phys. B **29**, 1530007 (2015).

[2] D. Leykam, A. Andreanov, and S. Flach, Artificial flat band systems: from lattice models to experiments, Adv. Phys.: X **3**, 1473052 (2018).

[3] N. Read, Compactly supported wannier functions and algebraic k-theory, Phys. Rev. B **95**, 115309 (2017).

[4] O. Derzhko and J. Richter, Universal low-temperature behavior of frustrated quantum antiferromagnets in the vicinity of the saturation field, Eur. Phys. J. B **52**, 23 (2006).

[5] O. Derzhko, J. Richter, A. Honecker, M. Maksymenko, and R. Moessner, Low-temperature properties of the hubbard model on highly frustrated one-dimensional lattices, Phys. Rev. B **81**, 014421 (2010).

[6] M. Hyrkäs, V. Apaja, and M. Manninen, Many-particle dynamics of bosons and fermions in quasi-one-dimensional flat band lattices, Phys. Rev. A **87**, 023614 (2013).

[7] A. Mielke, Ferromagnetism in the hubbard model on line graphs and further considerations, J. Phys. A: Math. Gen. **24**, 3311 (1991).

[8] H. Tasaki, Ferromagnetism in the Hubbard Models with Degenerate Single-Electron Ground States, Phys. Rev. Lett. **69**, 1608 (1992).

[9] T. Misumi and H. Aoki, New class of flat band models on tetragonal and hexagonal lattices: Gapped versus crossing flat bands, Phys. Rev. B **96**, 155137 (2017).

[10] S. Nishino and M. Goda, Three-dimensional flat band models, J. Phys. Soc. Jpn. **74**, 393 (2005).

[11] Elliott H. Lieb, Two Theorems on the Hubbard Model, Phys. Rev. Lett. **62**, 1201 (1989).

[12] A. Mielke, Ferromagnetic ground states for the hubbard model on line graphs, J Phys. A: Math. Gen. **24**, L73 (1991).

[13] A. Mielke, Exact results for the u= infinity hubbard model, J. Phys. A: Math. Gen. **25**, 6507 (1992).

[14] U. Brandt and A. Giesekus, Hubbard and Anderson Models on Perovskitelike Lattices: Exactly Solvable Cases, Phys. Rev. Lett. **68**, 2648 (1992).

[15] A. Ramachandran, A. Andreanov, and S. Flach, Chiral flat bands: Existence, engineering, and stability, Phys. Rev. B **96**, 161104(R) (2017).

[16] Y. Zong, S. Xia, L. Tang, D. Song, Y. Hu, Y. Pei, J. Su, Y. Li, and Z. Chen, Observation of localized flat band states in kagome photonic lattices, Opt. Express **24**, 8877 (2016).

[17] S. Mukherjee and R. R. Thomson, Observation of robust flat band localization in driven photonic rhombic lattices, Opt. Lett. **42**, 2243 (2017).

[18] S. Mukherjee and R. R. Thomson, Observation of localized flat band modes in a quasi-one-dimensional photonic rhombic lattice, Opt. Lett. **40**, 5443 (2015).

[19] R. A. Vicencio, C. Cantillano, L. Morales-Inostroza, B. Real, C. Mejía-Cortés, S. Weimann, A. Szameit, and M. I. Molina, Observation of Localized States in Lieb Photonic Lattices, Phys. Rev. Lett. **114**, 245503 (2015).

[20] S. Mukherjee, A. Spracklen, D. Choudhury, N. Goldman, P. Öhberg, E. Andersson, and R. R. Thomson, Observation of a Localized Flat Band State in a Photonic Lieb Lattice, Phys. Rev. Lett. **114**, 245504 (2015).

[21] N. Masumoto, N. Y. Kim, T. Byrnes, K. Kusudo, A. Löffler, S. Höfling, A. Forchel, and Y. Yamamoto, Exciton–polariton condensates with flat bands in a two-dimensional kagome lattice, New J. Phys. **14**, 065002 (2012).

[22] T. Jacqmin, I. Carusotto, I. Sagnes, M. Abbarchi, D. D. Solnyshkov, G. Malpuech, E. Galopin, A. Lemaître, J. Bloch, and A. Amo, Direct Observation of Dirac Cones and a Flatband in a Honeycomb Lattice for Polaritons, Phys. Rev. Lett. **112**, 116402 (2014).

[23] M. Biondi, E. P. L. van Nieuwenburg, G. Blatter, S. D. Huber, and S. Schmidt, Incompressible Polaritons in a Flat Band, Phys. Rev. Lett. **115**, 143601 (2015).

[24] S. Klembt, T. H. Harder, O. A. Egorov, K. Winkler, H. Suchomel, J. Beierlein, M. Emmerling, C. Schneider, and S. Höfling, Polariton condensation in S- and P-flatbands in a two-dimensional Lieb lattice, Applied Phys. Lett. **111**, 231102 (2017).

[25] D. Guzmán-Silva, C. Mejía-Cortés, M. A. Bandres, M. C. Rechtsman, S. Weimann, S. Nolte, M. Segev, A. Szameit, and R. A. Vicencio, Experimental observation of bulk and edge transport in photonic Lieb lattices, New J. Phys. **16**, 063061 (2014).

[26] S. Weimann, L. Morales-Inostroza, B. Real, C. Cantillano, A. Szameit, and R. A. Vicencio, Transport in sawtooth photonic lattices, Opt. Lett. **41**, 2414 (2016).

[27] S. Xia, Y. Hu, D. Song, Y. Zong, L. Tang, and Z. Chen, Demonstration of flat band image transmission in optically induced lieb photonic lattices, Opt. Lett. **41**, 1435 (2016).

[28] S. Taie, H. Ozawa, T. Ichinose, T. Nishio, S. Nakajima, and Y. Takahashi, Coherent driving and freezing of bosonic matter wave in an optical Lieb lattice, Sci. Adv. **1** e1500854 (2015).

[29] G.-B. Jo, J. Guzman, C. K. Thomas, P. Hosur, A. Vishwanath, and D. M. Stamper-Kurn, Ultracold Atoms in a Tunable Optical Kagome Lattice, Phys. Rev. Lett. **108**, 045305 (2012).

[30] F. Baboux, L. Ge, T. Jacqmin, M. Biondi, E. Galopin, A. Lemaître, L. Le Gratiet, I. Sagnes, S. Schmidt, H. E. Türeci, A. Amo, and J. Bloch, Bosonic Condensation and

Disorder-Induced Localization in a Flat Band, Phys. Rev. Lett. **116**, 066402 (2016).
[31] J. Vidal, P. Butaud, B. Douçot, and R. Mosseri, Disorder and interactions in Aharonov-Bohm cages, Phys. Rev. B **64**, 155306 (2001).
[32] J. T. Chalker, T. S. Pickles, and P. Shukla, Anderson localization in tight-binding models with flat bands, Phys. Rev. B **82**, 104209 (2010).
[33] D. Leykam, J. D. Bodyfelt, A. S. Desyatnikov, and S. Flach, Localization of weakly disordered flat band states, Eur. Phys. J. B **90**, 1 (2017).
[34] J. D. Bodyfelt, D. Leykam, C. Danieli, X. Yu, and S. Flach, Flatbands Under Correlated Perturbations, Phys. Rev. Lett. **113**, 236403 (2014).
[35] C. Danieli, J. D. Bodyfelt, and S. Flach, Flat band engineering of mobility edges, Phys. Rev. B **91**, 235134 (2015).
[36] R. Khomeriki and S. Flach, Landau-Zener Bloch Oscillations with Perturbed Flat Bands, Phys. Rev. Lett. **116**, 245301 (2016).
[37] A. R. Kolovsky, A. Ramachandran, and S. Flach, Topological flat Wannier-Stark bands, Phys. Rev. B **97**, 045120 (2018).
[38] J.-W. Rhim, K. Kim, and B.-J. Yang, Quantum distance and anomalous landau levels of flat bands, Nature (London) **584**, 59 (2020).
[39] C. Danieli, A. Maluckov, and S. Flach, Compact discrete breathers on flat band networks, Low Temp. Phys. **44**, 678 (2018).
[40] M. Johansson, U. Naether, and R. A. Vicencio, Compactification tuning for nonlinear localized modes in sawtooth lattices, Phys. Rev. E **92**, 032912 (2015).
[41] B. Real and R. A. Vicencio, Controlled mobility of compact discrete solitons in nonlinear lieb photonic lattices, Phys. Rev. A **98**, 053845 (2018).
[42] J. Vidal, B. Douçot, R. Mosseri, and P. Butaud, Interaction Induced Delocalization for Two Particles in a Periodic Potential, Phys. Rev. Lett. **85**, 3906 (2000).
[43] B. Douçot and J. Vidal, Pairing of Cooper Pairs in a Fully Frustrated Josephson-Junction Chain, Phys. Rev. Lett. **88**, 227005 (2002).
[44] M. Tovmasyan, S. Peotta, L. Liang, P. Törmä, and S. D. Huber, Preformed pairs in flat bloch bands, Phys. Rev. B **98**, 134513 (2018).
[45] C. Danieli, A. Andreanov, T. Mithun, and S. Flach, Quantum caging in interacting many-body all-bands-flat lattices, arXiv:2004.11880 [cond-mat.quant-gas].
[46] C. Danieli, A. Andreanov, and S. Flach, Many-body flatband localization, Phys. Rev. B **102**, 041116(R) (2020).
[47] Y. Kuno, T. Orito, and I. Ichinose, Flat band many-body localization and ergodicity breaking in the Creutz ladder, New J. Phys. **22**, 013032 (2020).
[48] T. Orito, Y. Kuno, and I. Ichinose, Exact projector hamiltonian, local integrals of motion, and many-body localization with symmetry-protected topological order, Phys. Rev. B **101**, 224308 (2020).
[49] A. Mielke and H. Tasaki, Ferromagnetism in the Hubbard model, Comm. Math. Phys. **158**, 341 (1993).
[50] H. Tasaki, Hubbard model and the origin of ferromagnetism, Eur. Phys. J. B **64**, 365 (2008).
[51] H. Tasaki, Stability of Ferromagnetism in the Hubbard Model, Phys. Rev. Lett. **73**, 1158 (1994).
[52] M. Maksymenko, A. Honecker, R. Moessner, J. Richter, and O. Derzhko, Flat Band Ferromagnetism as a Pauli-Correlated Percolation Problem, Phys. Rev. Lett. **109**, 096404 (2012).
[53] A. Mielke, Pair formation of hard core bosons in flat band systems, J. Stat. Phys. **171**, 679 (2018).
[54] S. Peotta and P. Törmä, Superfluidity in topologically nontrivial flat bands, Nature Commun. **6**, 8944 (2015).
[55] A. Julku, S. Peotta, T. I. Vanhala, D.-H. Kim, and P. Törmä, Geometric Origin of Superfluidity in the Lieb-Lattice Flat Band, Phys. Rev. Lett. **117**, 045303 (2016).
[56] R. Mondaini, G. G. Batrouni, and B. Grémaud, Pairing and superconductivity in the flat band: Creutz lattice, Phys. Rev. B **98**, 155142 (2018).
[57] G. E. Volovik, Graphite, graphene, and the flat band superconductivity, JETP Lett. **107**, 516 (2018).
[58] R. G. Dias and J. D. Gouveia, Origami rules for the construction of localized eigenstates of the Hubbard model in decorated lattices, Sci. Rep. **5**, 16852 EP (2015).
[59] L. Morales-Inostroza and R. A. Vicencio, Simple method to construct flat band lattices, Phys. Rev. A **94**, 043831 (2016).
[60] M. Röntgen, C. V. Morfonios, and P. Schmelcher, Compact localized states and flat bands from local symmetry partitioning, Phys. Rev. B **97**, 035161 (2018).
[61] S. Nishino, M. Goda, and K. Kusakabe, Flat bands of a tight-binding electronic system with hexagonal structure, J. Phys. Soc. Jpn **72**, 2015 (2003).
[62] J.-W. Rhim and B.-J. Yang, Classification of flat bands according to the band-crossing singularity of bloch wave functions, Phys. Rev. B **99**, 045107 (2019).
[63] S. Flach, D. Leykam, J. D. Bodyfelt, P. Matthies, and A. S. Desyatnikov, Detangling flat bands into Fano lattices, Europhys. Lett. **105**, 30001 (2014).
[64] W. Maimaiti, A. Andreanov, H. C. Park, O. Gendelman, and S. Flach, Compact localized states and flat band generators in one dimension, Phys. Rev. B **95**, 115135 (2017).
[65] W. Maimaiti, S. Flach, and A. Andreanov, Universal $d = 1$ flat band generator from compact localized states, Phys. Rev. B **99**, 125129 (2019).
[66] S. E. Palmer and J. T. Chalker, Quantum disorder in the two-dimensional pyrochlore heisenberg antiferromagnet, Phys. Rev. B **64**, 094412 (2001).
[67] B. Canals, From the square lattice to the checkerboard lattice: Spin-wave and large-n limit analysis, Phys. Rev. B **65**, 184408 (2002).
[68] M. Mekata, Kagome: The Story of the Basketweave Lattice, Phys. Today **56**, 12 (2003).
[69] I. Syôzi, Statistics of Kagomé Lattice, Prog. Theor. Phys. **6**, 306 (1951).
[70] R. Bistritzer and A. H. MacDonald, Moiré bands in twisted double-layer graphene, Proc. Natl. Acad. Sci. **108**, 12233 (2011).
[71] G. Tarnopolsky, A. J. Kruchkov, and A. Vishwanath, Origin of Magic Angles in Twisted Bilayer Graphene, Phys. Rev. Lett. **122**, 106405 (2019).

[72] H. Ha and B.-J. Yang, Macroscopically degenerate localized zero-energy states of quasicrystalline bilayer systems in strong coupling limit, arXiv:2103.08851 [cond-mat.mes-hall].

[73] Z.-H. Yang, Y.-P. Wang, Z.-Y. Xue, W.-L. Yang, Y. Hu, J.-H. Gao, and Y. Wu, Circuit quantum electrodynamics simulator of flat band physics in a Lieb lattice, Phys. Rev. A **93**, 062319 (2016).

[74] Z. Li, J. Zhuang, L. Wang, H. Feng, Q. Gao, X. Xu, W. Hao, X. Wang, C. Zhang, K. Wu, S. X. Dou, L. Chen, Z. Hu, and Y. Du, Realization of flat band with possible nontrivial topology in electronic kagome lattice, Sci. Adv. **4** (2018).

[75] W. Yan, H. Zhong, D. Song, Y. Zhang, S. Xia, L. Tang, D. Leykam, and Z. Chen, Flatband line states in photonic super-honeycomb lattices, Adv. Opt. Mater. **8**, 1902174 (2020).